RSC Advances

REVIEW

View Article Online
View Journal | View Issue

Check for updates

Cite this: *RSC Adv.*, 2021, **11**, 21904

Recent advances in the metal–organic framework-based electrocatalysts for the hydrogen evolution reaction in water splitting: a review

Neelam Zaman,[a] Tayyaba Noor [b] and Naseem Iqbal *[a]

Received 21st March 2021
Accepted 9th June 2021

DOI: 10.1039/d1ra02240g

rsc.li/rsc-advances

Water splitting is an important technology for alternative and sustainable energy storage, and a way for the production of hydrogen without generating pollution. In recent years, metal–organic frameworks (MOFs) have become the most capable multifunctional resources because of their high surface areas, tunable porosity, simple modification of compositions, and potential for use as precursors with a variety of morphological structures. Based on these qualities, many MOFs and their derived materials are utilized as electrocatalysts for the water splitting reaction. Herein, we assembled the relevant literature in recent years about MOF and MOF-derived materials for their eminent electrocatalytic activity in water splitting with useful strategies for the design and preparation of catalysts, along with challenges. This review summarizes the advancement in MOF materials, elucidating different strategies for its role in water splitting.

Open Access Article. Published on 21 June 2021. Downloaded on 2/3/2026 10:12:05 PM.
This article is licensed under a Creative Commons Attribution-NonCommercial 3.0 Unported Licence.

1. Introduction

At present, the environmental pollution and energy disaster are of global concerns. To ensure a green and sustainable future, an alternative renewable energy source is needed to replace our dependence on fossil fuels. Nowadays, hydrogen as an energy source is of great interest because of several remarkable qualities, such as its renewable nature, elevated gravimetric energy (~142 MJ kg^{-1}) and combustion product with no greenhouse gas emission. Hydrogen as a fuel can power vehicles based on the hydrogen fuel cell due to its extraordinary energy efficiency. In contrast to combustion engines fueled by gas, hydrogen fuel cells show 2 to 3 times more efficiency with no harmful by-products. It only generates warm air and water vapor, and also has the capability for growth in the transportation and stationary energy sectors.[1]

An eco-friendly way of hydrogen production is the splitting of water by a variety of ways, *i.e.*, by the electrochemical way of splitting, by the chemo-catalytical way of splitting, and also by the photocatalytic way,[2] that provide a better way to obtain highly pure hydrogen.[2,3] However, hydrogen production *via* electrochemical method is hampered by three central limitations such as (i) the short lifetime of the electrode material, (ii) the lack of cost-effective alternatives for noble metals, and (iii) the thermal efficiency, which is lower than the water splitting thermodynamic limits, *i.e.*, 1.23 V.[4]

The hydrogen evolution reaction (HER) has now attracted great attention, owing to remarkable features: (a) it provides pure hydrogen, and (b) in the future, is considered as an appealing energy carrier contender for the fuel cell.[5] As we already know, these reactions are carried out in acidic and alkaline media, and research has been carried out on many less expensive metal catalysts. However, it should be noted that many metal catalysts show inadequate stability in acidic media.[6] Moreover, noble metal catalysts are preferred in acidic media, but other catalytic materials (such as oxides of Ir and Ru and carbides of tungsten) are also employed for HER in acidic media.

On the contrary, electrolysers based on alkaline media are technically well developed and widely available on the commercial scale. Moreover, the hydrogen evolution reaction in alkaline media presents an attractive substitution that not only enhances the stability of noble metal-based catalysts, but also opens a new way of investigating inexpensive metal (transition metals) utilization as catalysts for HER. Moreover, in alkaline media, HER is controlled *via* three elusive and significant descriptors, such as (i) hydrogen adsorption on the catalysts surface, (ii) preclusion of the adsorption of the hydroxyl group on the catalyst surface as they poison the active sites of the catalysts used, and (iii) the energy needed for water molecule dissociation.[7] However, the main challenge in alkaline-based HER technology is the decreased kinetics of the reaction.[8] Thus, a new catalyst is needed that has the following features: (i) may overcome the additional energy requirements for water molecules dissociation, (ii) moderates the affinity of hydrogen adsorption and its recombination to yield the hydrogen gas, and (iii) prompts the kinetics of the reaction.[9]

Like other evolution reactions, it requires a high overpotential; therefore, it is imperative to find a suitable electrocatalyst that considerably exploits the efficiency of the process.[10] In this regard, noble metals (like platinum, ruthenium and

[a]*U.S.-Pakistan Centre for Advanced Studies in Energy (USPCAS-E), National University of Sciences and Technology (NUST), H-12 Campus, Islamabad 44000, Pakistan. E-mail: naseem@uspcase.nust.edu.pk; Tel: +92 51 9085 5281*

[b]*School of Chemical and Materials Engineering (SCME), National University of Sciences and Technology (NUST), H-12 Campus, Islamabad 44000, Pakistan*

© 2021 The Author(s). Published by the Royal Society of Chemistry

Open Access Article. Published on 21 June 2021. Downloaded on 2/3/2026 10:12:05 PM.
This article is licensed under a Creative Commons Attribution-NonCommercial 3.0 Unported Licence.

palladium) are ideal electrocatalysts for HER. However, due to their scarcity and high cost, it is urgent for the current electrochemical research area to find an inexpensive electrocatalyst. Many metals for HER have also been investigated in alkaline and acidic media in the last few decades.[11] Predominantly, 20% Pt/C is typically used as a HER electrocatalyst and considered as the benchmark catalyst, and most of the research has been focused on preparing catalysts that show even better performance. In this regard, many non-precious metal-based catalysts are prepared, such as transition metal-based sulphides, nitrides and oxides, but their performance is far from that of the precious metal-based catalysts because of their limited flexibility in catalyst design and reduced porosity.[12]

Consequently, a new family of porous solids called porous coordination polymer or metal–organic framework stand out as a highly efficient candidate for HER. They are characterized by the maximum degree of crystallinity, porosity, a high surface area and pore size that clearly go beyond that of other porous materials. As a catalyst, the development of MOF has attracted the attention of researchers over the past decade and followed two essential strategies: first, by carefully overlapping the orbital of the molecular component for the design of MOF conductive and semiconductive forms.[13] Second, the development of redox active MOFs from the components that allow the charge of the electron and hole to jump. During its development, the primary goal is to develop a low energy band gap, as at the fundamental level, it offers an easy charge transfer in coordination with space.[14]

Similarly, the synergistic effect of the MOFs framework and its porous properties has provided a new range of applications of these MOFs in a widespread range of fields, particularly in catalysis. It is compulsory to note the outer coordination sphere effects of the MOFs-based catalysts, such as hydrogen bonding and proton transfer transmit. This leads to the assumption that the MOFs catalytic sites could be approached *via* the engineering of its frameworks by incorporating various active ligands and metal components, and can present very astonishing synergetic effects, which will lead to much improved catalytic activity. However, as precursors, MOFs can produce a variety of metal compounds or metal and carbon composites with deliberate consideration of the elemental structures and compositions.[15]

Taking advantage of the high surface area and porosity of the MOFs, it has been employed as a catalyst for HER in the last few decades.[16] In addition, it has been used as an electrocatalyst for HER because of the following reasons: (i) to replace the expensive metal-based catalysts (PGM) with low-cost metals, (ii) for lowering the needed overpotential during HER, (iii) for escalating the kinetics of the reaction.[17] Moreover, the surface area, porosity and stability of the MOF-based materials are further enhanced by composite formation with graphene oxide, reduced graphene oxide and carbon nanotube. It not only enhances the surface area and porosity, but also boosts the activity of MOF in the water splitting reactions.[18]

Still, there are very few surveys on catalysts based on MOFs that thoroughly explain the mechanism of catalysing HER, cover up MOF supports, pristine MOFs and derived products of MOFs for HER. Thereby, this report is intended for recapitulating the current progress made in MOFs-based catalysts, and three forms of the hydrogen evolution reaction with a thorough explanation of the mechanisms of reinforced activity and for their material handling. In addition, this review will discuss the probable modifications in the morphologies and electronic structures of the electrocatalysts, for tuning their active sites, and stable performances as competent catalysts for HER. First, we will explain the fundamentals and electrochemistry of HER in alkaline and acidic media. Then, we will outline the requirements for an efficient and stable catalyst, challenges with HER and limitations of electrocatalysts, along with prospective solutions and recently reported data in detail. At the end, we will list the concluding remarks.

2. Fundamentals of HER in acidic and alkaline media

2.1 Reaction mechanism in acidic and alkaline media

A substitute of clean fuel for various energy systems and the development of hydrogen through the hydrogen evolution reaction in alkaline medium is currently a point of focus. This process suffers from sluggish kinetics due to an additional water dissociation step. So, the modern catalysts perform well in an acidic medium and loses significant catalytic performance in alkaline medium.[19]

Theoretical studies have shown that the performance of the catalyst in an alkaline medium is mainly controlled by two factors. These factors are water dissociation and hydrogen binding energy. Thus, any catalyst having better capability to dissociate the water molecules with good binding capacity and produce a hydrogen molecule will result in better HER catalysis in an alkaline medium.[20] In terms of the reaction efficiency, very few electrocatalysts have been reported that have competence with Pt in an alkaline medium. Therefore, the basic laws of electrode kinetics should be verified, and the reaction mechanism needs to be explored. This will provide a foundation for new researchers to examine new and efficient electrocatalysts.[21]

The catalytic reactions follow different mechanisms, as shown in Fig. 1. In an acidic medium, the reaction follows the combination of an electron from the electrode surface and a proton from the electrolyte, which is stated as the Volmer pathway. Another combination of the existing hydrogen atom with the adjacent one is referred to as the Tafel pathway. The combination of another proton from the electrolyte and an electron from the electrode surface is referred to as the Heyrovsky pathway. On the other hand, in alkaline media, the protons are absent in electrolytes. So, the reaction starts from the dissociation of a water molecule, referred to as the Volmer pathway. Then, either the Tafel or Heyrovsky pathway follows for hydrogen production. The additional water dissociation step in the alkaline electrolyte indicates that the same catalyst shows worse performance in an alkaline solution than in acidic medium.[22] Moreover, the H_2 electrocatalytic evolution (HER) on the surface of the catalyst-deposited electrode can be explained in terms of the mechanism. The HER in the alkaline solution is

Open Access Article. Published on 21 June 2021. Downloaded on 2/3/2026 10:12:05 PM.
This article is licensed under a Creative Commons Attribution-NonCommercial 3.0 Unported Licence.

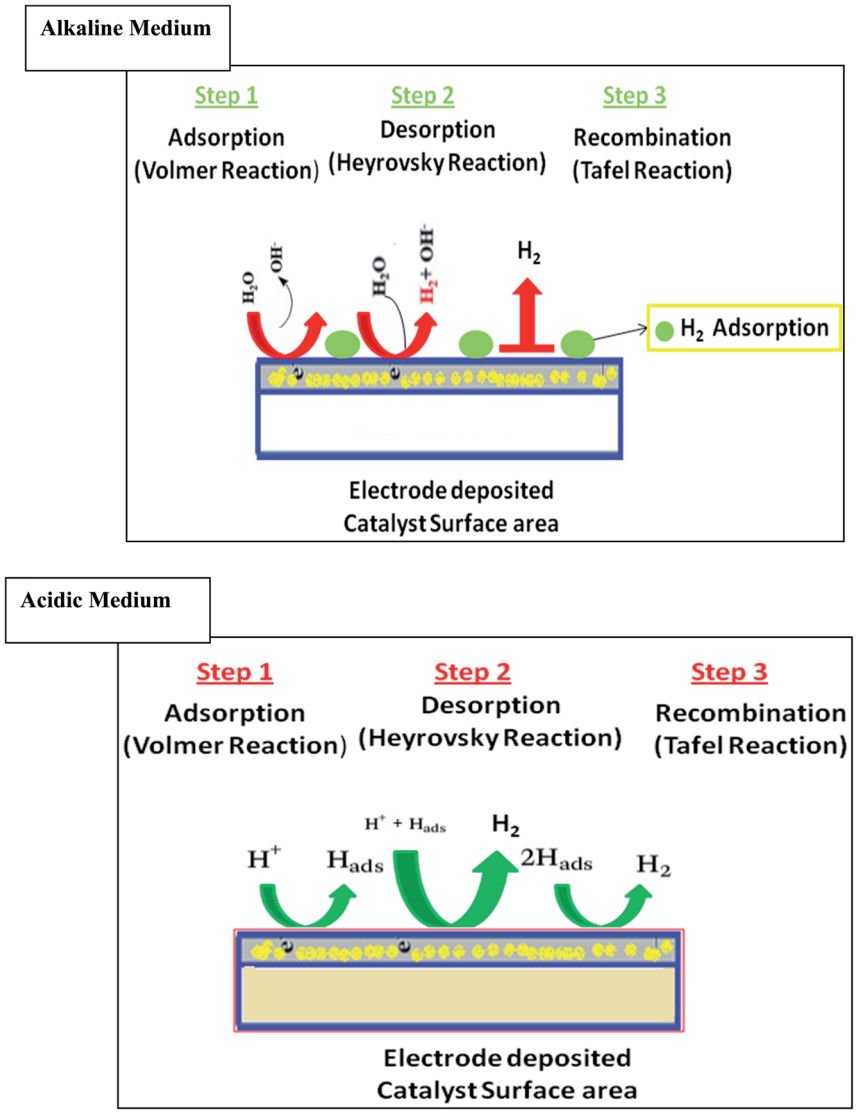

Fig. 1 Schematic diagram of the Volmer–Heyrovsky and Volmer–Tafel processes on a catalyst surface in acidic and alkaline media.

considered a combination of three basic steps, one chemical and two electrochemical. It can be seen that the initial step is an electrochemical reduction of water to give a hydrogen molecule, adsorbed on the electrode surface by the Volmer reaction. Then, there is an electrochemical step for the adsorbed hydrogen to produce H_2, followed by the Heyrovsky reaction or by chemical reaction, *i.e.*, Tafel reaction.[23]

In addition, the Tafel slope values define the potential difference required to increase or decrease the current density by 10-fold, which shows the HER process mechanism. When the Volmer or discharge reaction is fast and the rate-determining step is the chemical desorption (combination), the b should be 29 mV dec^{-1} and given by $b = 2.3RT/2F = 0.029$ V dec^{-1} at 25 °C. However, if the discharge reaction is fast and the rate-determining step is the electrochemical desorption, *i.e.*, Heyrovsky reaction, then the b should be 39 mV dec^{-1} and set by $b = 2.3RT/2F = 0.039$ V dec^{-1} at 25 °C. Finally, if the discharge reaction is slow, then the b should be 116 mV dec^{-1} and given by $b = 2.3RT/2F = 0.116$ V dec^{-1} at 25 °C.

Volmer reaction

$$M + H_2O + e^- \rightleftharpoons MH_{ads} + OH^- \quad (1)$$

Heyrovsky reaction

$$MH_{ads} + H_2O + e^- \rightleftharpoons H_2\uparrow + M + OH^- \quad (2)$$

Tafel reaction

$$MH_{ads} + MH_{ads} \rightleftharpoons H_2\uparrow + 2M \quad (3)$$

2.2 Rate of reaction

The hydrogen adsorption free energy, ΔG_H, mainly determines the rate of the overall reaction. If the hydrogen molecule weakly binds the catalyst surface, then the adsorption (Volmer) step will limit the overall reaction rate. Whereas if the hydrogen

© 2021 The Author(s). Published by the Royal Society of Chemistry

Open Access Article. Published on 21 June 2021. Downloaded on 2/3/2026 10:12:05 PM.
This article is licensed under a Creative Commons Attribution-NonCommercial 3.0 Unported Licence.

binds catalyst surface is too strong, then the desorption, *i.e.*, Heyrovsky/Tafel step will limit the rate. Thus, for an active HER catalyst, $\Delta G_H \approx 0$ is the necessary (but inadequate) condition. One of the characteristics of an active catalyst is that it neither binds the reaction intermediate too strongly, nor too weakly.

2.3 The volcano plots

To modify the HER catalyst in acidic medium, the volcano plots have been used as a guiding principle. This predicts that metals with an optimal H-binding energy will be at the top of the volcano, such as the PGMs, and will show the highest activity. The optimal binding energy defines neither poor adsorption of the reactants, nor exertion in the desorption of the final product. Similar to the case in acidic medium, Yan and co-workers recently revealed that the relation between the HER exchange current density in alkaline medium and H-binding energy values can be linked *via* a volcano type of relationship. This is supported by both experimental and DFT studies.

Primarily, the HER activities on a series of non-metallic surfaces are studied by different electrochemical measurements, such as cyclic voltammetry (CV) on a Pt surface and linear sweep voltammetry (LSV) on non-Pt surfaces. The exchange current densities $\log(j_0)$, roughness factor and Tafel slopes were correlated. Afterwards, DFT calculations were applied, and H-binding energy values were calculated *via* the Vienna *ab initio* simulation package. Upon further discovering a relationship between the HER activity and H-binding energy, similar volcano plots were schemed that set the HER exchange current density as a function of the calculated H-binding energy values of these metallic surfaces. In acidic media, Pt (still at the top of the volcano plot) requires minor overpotentials to get high value reaction rates. However, the cost and insufficiency of Pt limits its extensive use; thus, there is a need to search for earth-abundant catalysts that have the capacity to substitute Pt.[24] Other metals like W, Fe, Ni, Co, and Pd have high H-binding energy in acidic media. In accordance with the d-band centre theory, the adsorption phenomenon is stronger when the d-band centre is adjacent to the Fermi level and displays weak adsorption when the Fermi level and d-band centre are at a distance. Therefore, 3d transition metals, *e.g.*, Fe, Co, Ni, are mixed with Pt to make an alloy, and this addition could alter the electronic properties and coordination environment of Pt. The utilization of Pt in this way is a better approach.[25]

In alkaline media, the activity of HER drops by many fractions as the value of the H-binding energy of Pt differs in the acidic solution volcano curve. This suggests that the H-binding energy might be a valuable criterion for recognizing the HER electrocatalyst. The HER performance can be enhanced by regulating the chemical properties of the surface for the optimal value of the H-binding energy. Despite that, Stechmickler and co-workers recently clarified that once the oxide covers the surface of the metal, *i.e.*, Mo, Ti and W, the relevancy of the volcano plots vanished. The oxide layer drops the activity. So, it was decided that Sabatier's principle predominantly resolved the reaction, with exception of Ni and Co. These are 3d metals having concise and small imbrication with hydrogen, that marks them as worthy catalysts. The rate of the reaction decreases for other metals because of the vastly exothermic hydrogen adsorption and its complex pathway, which is the result of many reaction intermediate stages. Hence, a worthy catalyst should reach one of these three criteria: (i) it is necessity to follow Sabatier's principle, *i.e.*, at the equilibrium potential $\Delta G \approx 0$, (ii) it is better to possess a d-band to extend over the Fermi level, and (iii) a distance of 0.5 Å is required as the electron relocates from the active catalyst, *i.e.*, adsorption site, to the proton. Consequently, catalysts possessing strong collaboration between the hydrogen 1s orbital and the d-band will be recommended (Fig. 2).

2.4 Requirements of catalysts for HER

The HER standard reduction potential is 0 V *vs.* RHE (at a standard temperature of 25 °C and pressure, 1 atm). Nevertheless, a higher applied potential is mandatory for the actual process of water electrolysis because of the association of the ion transfer and complex electron processes. This causes a low effeciency and slow kinetics.[26]

The performance of the electrocatalysts is typically evaluated by the subsequent parameters.[27]

2.4.1 Overpotential. A catalyst that is worthy for HER should have the capacity to lower the overpotential because a low overpotential value is the reason for high catalytic activity. The theoretical value of the cell potential for the complete water splitting route is 1.23 V (1.23 V for the oxygen evolution reaction (OER) and 0 V for HER). The OER and HER both require extra potential to recruit reactions due to obstacles. One of the crucial factors to estimate the catalyst activity is the extra potential, *i.e.*, overpotential (η). Usually, overpotential values of different catalysts are related at a fixed current density, such as 100 mA cm^{-2} ($\eta = 100$) and/or 10 mA cm^{-2} ($\eta = 10$). The preferred HER catalyst should be capable of catalysing the reaction between 100 mV and less.

2.4.2 Electrochemically active surface area (ECSA). The electrode material active area can reach the electrolyte for its

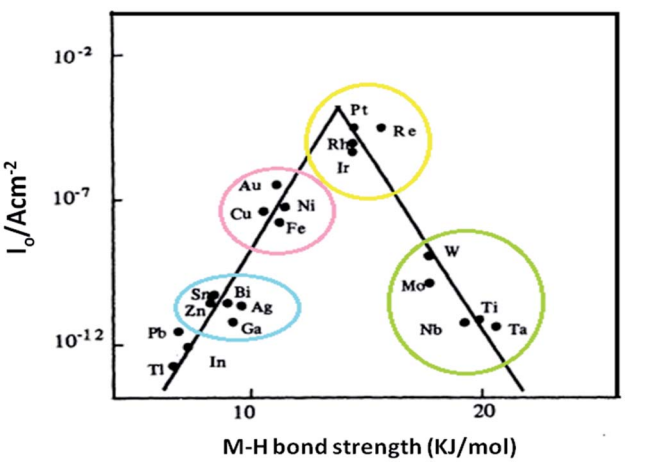

Fig. 2 Volcano plot of the exchange current density *vs.* metal–hydride bond strength.

Open Access Article. Published on 21 June 2021. Downloaded on 2/3/2026 10:12:05 PM.
This article is licensed under a Creative Commons Attribution-NonCommercial 3.0 Unported Licence.

charge transfer. Various techniques can be used to expand the electrode surface area. This includes nano structuring, cyclic voltammetry (for total electrode activity), and linear sweep voltammetry (LSV). The steady-state currents at several applied voltages can be adapted to define the accurate catalytic activity with a limited time of 5 minutes.

2.4.3 Faradaic efficiency. Another parameter to evaluate the act of the electrocatalyst is the faradaic efficiency (FE). This is adapted to estimate the number of electrons in the desired reaction in place of the side reaction. FE is the ratio of the quantity of experimentally identified H_2 to the theoretical amount of H_2, which is intended from the current density built on 100% faradaic revenue. This is the ratio of the experimentally developed amount of H_2 to the theoretical H_2 quantity in the HER process. Gas chromatography (GC) or water displacement technique can be adapted to estimate the amount of produced H_2. The theoretical scheming of H_2 is done by the circumstances of potentiostatic or galvanostatic electrolysis, and relating it with an experimental value permits us to determine the faradaic efficiency. In general, 100% FE is reported in HER and a greater FE signifies enhanced astuteness for the HER process in alkaline media.

2.4.4 Turnover frequency. The turnover frequency specifies the number of reactants converted by the catalyst, per catalytic site, to the preferred product in per unit time. At present, the scheme that is mostly intended for the HER catalyst TOF values is centred on TOF $= jA/4nF$, where A represents the area of the working electrode and n embodies the active material number of moles, designed from the surface area of the catalyst, which is electrochemically active. Nevertheless, it is not easy to find accurate TOF values for most of the solid-state catalysts, mainly for the few evolving complexes. The reason is that all of the surface atoms of the catalyst are not equally reachable or catalytically active. Furthermore, bubbles are produced with HER on the electrode surface, resulting in an increase of the overpotential because of the damage of the active surface area. The TOF values are inexact, but they still can be beneficial to relate the catalytic activity of several catalysts, mainly with the indistinguishable system case.[28]

2.4.5 Hydrogen bonding energy. An ideal electrocatalyst for HER should not display too strong or too weak HBE. The HER process shows that the first proton diffuses, and is then linked to the surface of the electrocatalyst, and is finally reduced to H_2. Instead, the weak HBE indicates that the adsorbed proton concentration on electrocatalyst is small. The catalysts become poison when the HBE is strong because the catalyst active sites are always covered with adsorbed H^+. The standard hydrogen electrode is taken at zero, so for an ideal HER electrocatalyst, the value of ΔG_{H^*} is compelled to zero. The current density is also very important to describe the performance of HER. Consequently, the HER improved activity is exhibited by electrocatalysts that are close to the top of the Sabatier volcano curve.[29]

2.4.6 Stability. The stability is another significant indicator for HER catalyst utilization. For stability evaluation, there are two approaches. One is monotonous cyclic voltammetry (CV) or linear sweep voltammetry (LSV), and another is potentiostatic or galvanostatic electrolysis. This voltammetric method, by performing the CV or LSV in the section together with the onset potential, is used to compare the amendments in the overpotential, before and after a definite run of cycles (*e.g.*, 10.000). After manifold potential cycling, a slight modification in the overpotential suggests that the electrolysis is well-balanced. For monitoring the potential (or current) divergence with time, at a constant current density of the electrocatalyst, galvanostatic or potentiostatic approaches are used and the applied current density must be at a minimum of 10 mA cm^{-2} and the period should last for at least 10 h. For longer duration in the absence of potential or current variation recommended worthy stability.

3. Challenges associated with the HER electrocatalyst

In water splitting, the fundamental reaction is the hydrogen evolution reaction, which is of great interest in modern electrochemistry. This has attracted even more consideration throughout the past decades by the reason of the rising needs for renewable energy and for exploiting fuel cells as a green device for energy conversion. Therefore, to better explore the MOF and MOF-derived electrocatalysts for HER, there are subsequent urgent issues that need to be considered.

Presently, a number of MOF precursors have been independently investigated, usually of different dimensions (such as in 1D, 2D and 3D), while the mixing of different dimension-based precursor MOFs has rarely been reported. It is well known that a 3D MOF shows better stability in the morphology and structure with high porosity, but exhibits less active site utilization. In contrast to the 3D MOFs, another 1D/2D MOF shows better utilization of the active sites, but exhibits low stability in the structure and morphology, and also shows poor porosity. Thus, mixing the merits of the 3D MOF with the 1D/2D MOF is highly desired, but still remains a great challenge for researchers.[30]

Secondly, MOF and MOF-based composites as an electrocatalyst for HER show better performance, but at high temperature treatment they are easily collapsed, fused and form aggregates, which significantly lowers the exposure of the catalyst active sites and also lowers its mass transfer abilities. As a result, they exhibit lower electrocatalytic performances. To deal with these issues, there is a need of comparatively lower temperature treatment. However, low temperature treatments will lead to poor electrical conductivity due to the carbonization of organic groups at lower temperatures, which would show a low degree of graphitization of the carbon matrix. Thus, attaining an optimum balance between the particle distribution graphitization degree and surface structure within the MOF-based composite systems by means of a suitable temperature is still challenging.

Furthermore, most reports hardly discuss the stability of the MOFs-based catalysts under working conditions, and also ignore the degradation mechanism. Consequently, inclusive effort must be dedicated to exploring the fundamentals of the degradation activity, and there is also a need for developing very

© 2021 The Author(s). Published by the Royal Society of Chemistry

Open Access Article. Published on 21 June 2021. Downloaded on 2/3/2026 10:12:05 PM.
This article is licensed under a Creative Commons Attribution-NonCommercial 3.0 Unported Licence.

active MOF-based HER electrocatalysts that exhibit high electrocatalytic activity with long-term stability at different operating conditions.[31]

Moreover, for fabricating an astonishing electrocatalyst working in acidic or alkaline medium, there are challenges related to HER. Electrocatalysts working efficiently in acidic media are not proficient in alkaline media because a high overpotential is needed in the alkaline media to initiate the catalysis with deprived power efficiencies. Furthermore, the chemistry of these reactions suggests that an additional energy barrier is requisite, which needs to be overcome by the verity of the catalysts to carry on the hydrogen production electrocatalytically.

Besides the dissociation of water, the binding energy of water is poorer in contrast to the OH^- ion, and is an additional challenge to construct a metal hydrogen bond in alkaline media. Moreover, the surface coverage by spectator species even in the auxiliary HER potential region confines the logical prediction about the rate-controlling factors and their interaction.

In addition, there are debates regarding the rate of HER in high (pH = 13) and low (pH = 1) pH. In alkaline medium, the rate of the reaction is 2–3 times lower in magnitude than in acidic media. This is why in alkaline media, the reaction is more sensitive to the surface atom than in acidic media, where the reaction is highly insensitive to the surface atom. In the end, the question arises whether the HER activity on the metal surfaces in alkaline electrolytes can approach the activity in acidic medium, *i.e.*, at low pH values.[7b]

4. State of electrocatalysts for HER

Up to now, catalysts for HER in alkaline medium are reported to be lower in number than catalysts for acidic medium. Furthermore, in alkaline media, the HER catalysts can be categorized into three major groups, such as (i) the noble metals and their alloy-based catalysts, *e.g.*, Ir, Pt, Ag, Ru, Pd; (ii) low-cost transition metals and their heterogamous nanostructure-based catalysts, including Mn, Fe, Cu, Co, Mo, Ni, and W; and (iii) non-metal based catalysts consisting of B, P, C, N, S, and their alloys. Fig. 3a–c illustrates the activity of a few of the noble metal-based catalysts in acidic and alkaline media.

Nowadays, the research has been focused on developing HER MOF-based catalysts in alkaline medium with enhanced stability and high activity, and it is considered as an important and promising candidate for commercial viability.

Like previous cavernous catalysts, the pristine forms of MOFs or MOFs as supporting frameworks can be used to halt, scatter and remove external species that are catalytically active on account of their powerfully built and adaptable network. This blend of catalytically active nanoparticles with frameworks can initiate astonishing interactive effects. This would advance the functioning of either guest material or host. Nevertheless, as a precursor, MOFs can be employed to produce a diversity of metal components or composites of metal/carbon with purposefully planned elemental composition and structure. Recently, a significant number of articles have emerged on HER MOFs-based catalysts. Furthermore, in industries, an unpredictable expansion of hydrogen power-driven technologies has developed. However, the MOFs-based catalysts were revised thoroughly for characteristics, devices, manufacturing and their electrocatalysis employment. For example, Mehmood *et al.* in 2016 displayed a MOF-based materials review for electrocatalysis. This indicates the application of MOFs in all sorts of electrochemical applications, and in particular, electrocatalytic HER. Wang *et al.* in 2017 issued a thorough report of MOFs for its energy utilization. This covers fuel cells, CO_2 reduction, Li-ion batteries, chemical reservoirs and also water splitting/HER.

MOF-based HER catalysts demonstrate significant properties, such as elevated reaction kinetics, reduced overpotential, and for the hydrogen intermediate, their suitable Gibbs free energy. Regardless of its considerable properties, their continuing stability at eminent current density, *i.e.*, 500 mA cm^{-2}, is rare such that it obstructs their practical relevance in water electrolysis devices. Moreover, in many reports, its stability is scarcely discussed under working conditions, and its degradation mechanism is totally ignored. Therefore, a large effort should be directed to unveiling the basics of activity degradation and developing very active MOF-derived HER electrocatalysts with long-term stability at high current densities, as discussed below:

4.1 Pristine MOFs

Similar to other porous materials used as catalysts, the metal–organic framework can also be employed in pristine forms.[32] In designing pristine MOFs for the hydrogen evolution reaction, the choice of organic linkers and metal type is mostly based on the framework configuration and catalytic activity. However, as an electrocatalyst, it has rarely been applied for HER catalysis due to its low conductivity and proportional instability in alkaline and acidic media. In this regard, a number of steps have been taken for improving the catalytic activity of pristine MOFs for the hydrogen evolution reaction without the requirement of post-treatment. It includes MOF hybridization with active materials and its combination with highly conductive substrates, such as graphene oxide, reduced graphene oxide-activated carbon and others. Table 1 shows the list of pristine MOFs from the literature. However, some of the superlative successes are linked with the effective design of the catalyst framework itself, as described below.

Jahan *et al.* reported on the GO-based Cu-MOF catalyst for the hydrogen evolution reaction prepared *via* solvothermal reaction.[33] For HER, the catalyst is tested in an acidic medium (0.5 M H_2SO_4), and showed a potential of −0.209 V *vs.* RHE at the current density value of 30 mA cm^{-2} with a Tafel slope value of 84 mV dec^{-1}. These parameters are equivalent to the benchmark catalyst, *i.e.*, 20% Pt/C showing a potential of −0.058 V *vs.* RHE and Tafel slope of 30 mV dec^{-1}. The noted point is the current density of 30 mA cm^{-2}, which is considered by the authors to not be the benchmark current density value of 10 mA cm^{-2} due to their early year publication in 2013.

Open Access Article. Published on 21 June 2021. Downloaded on 2/3/2026 10:12:05 PM.
This article is licensed under a Creative Commons Attribution-NonCommercial 3.0 Unported Licence.

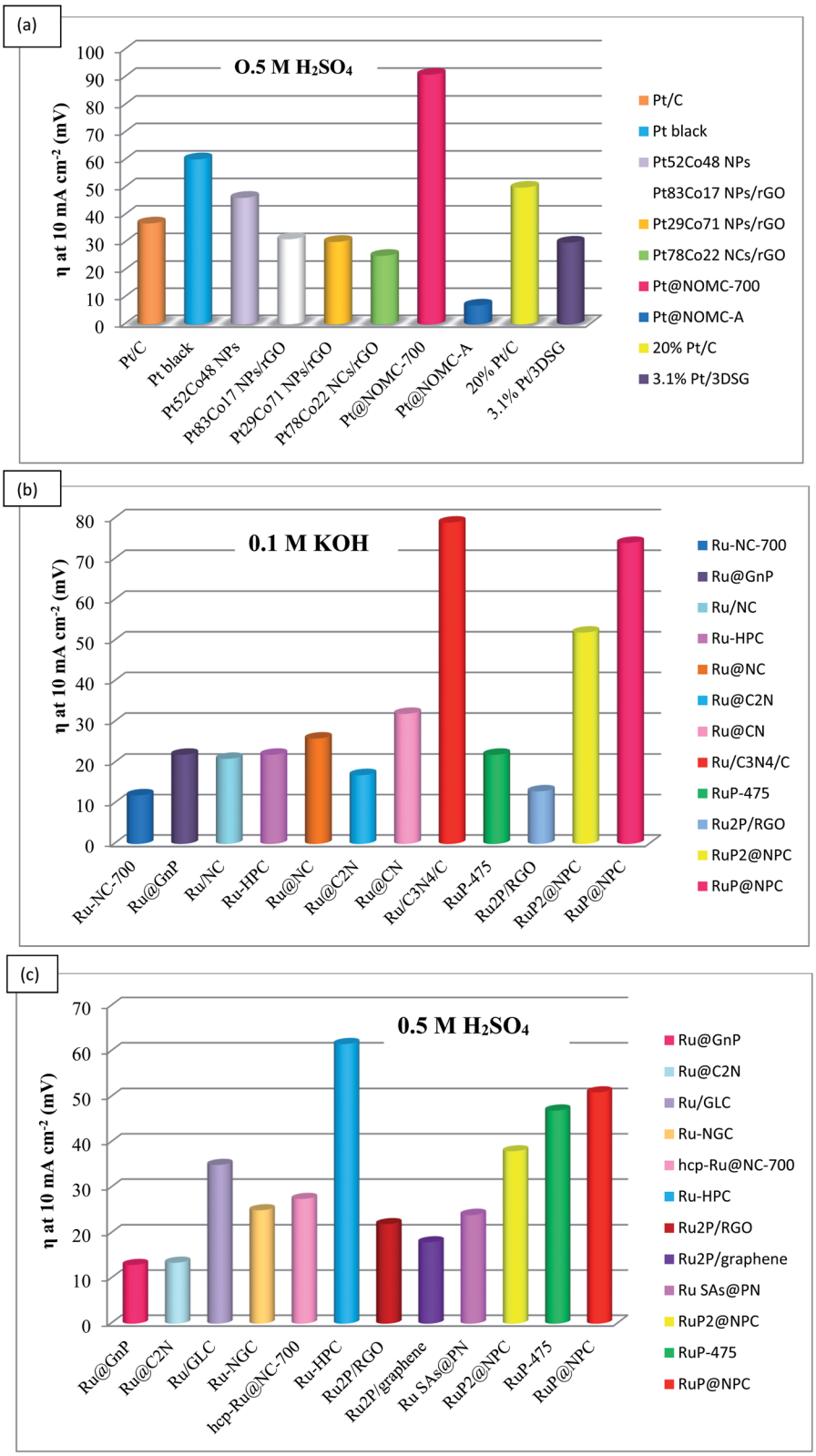

Fig. 3 Comparison of noble metal-based catalysts for HER in acidic and alkaline media. (a) Pt-based electrocatalysts; (b and c) Ru based electrocatalysts.

Subsequently, the overpotential value at a current density of 10 mA cm^{-2} is broadly accepted and employed as a comparison of various experimental results in the literature.

The choice of organic linkers and metal node is primarily based on their framework formation and its catalytic performance for HER, and considered as the significant part in the

© 2021 The Author(s). Published by the Royal Society of Chemistry

Open Access Article. Published on 21 June 2021. Downloaded on 2/3/2026 10:12:05 PM.
This article is licensed under a Creative Commons Attribution-NonCommercial 3.0 Unported Licence.

design of the pristine MOF as a catalyst for the electrocatalytic hydrogen evolution reaction.

Wu *et al.* reported an alternative pristine Co-based pristine MOF, such as CTGU-5 and CTGU-6. Initially, they are synthesized as a mixture by following the solvothermal method, but crystallized in the pure form by employing neutral and anionic surfactants, as illustrated in Fig. 4a. Both MOFs comprise cobalt as the metal, and 1,4-bis(imidazole)butane and naphthalene-1,4-dicarboxylic acid as the ligands. Both prepared MOFs are different from one another by the way they coordinate with the H_2O molecule. For example, in CTUG-5, the water molecule is coordinated with the central metal (*i.e.*, Co) part of MOF. In contrast, in CTUG-6, the water molecule is coordinated with the framework through hydrogen bonding. Due to these differences in the coordination, the following MOFs exhibits a 2D structure for CTUG-5 and 3D structure for CTUG-6.

Both prepared catalysts were used for HER in an acidic medium (0.5 M H_2SO_4). They exhibit the following Tafel slopes and onset potential values, such as 176 mV dec^{-1} and 425 mV for CTUG-6 and 125 mV dec^{-1} and 388 mV for CTUG-5, respectively. In addition, various acetylene black (AB)-based composites with varying stoichiometric ratios of acetylene black and CTUG-5 were prepared. The composite AB&CTGU-5(1 : 4) demonstrated superior electrocatalytic activity. At 10 mA cm^{-2}, it exhibited low overpotential up to 44 mV with 45 mV dec^{-1} (Tafel slope). At 255 mV overpotential, it showed stability for 96 h in chronoamperometric performance.

At the end, it can be summarized that in the pristine MOF, the choice of metal can determine the electrocatalytic activity for HER. In addition, the choice of organic linker is crucial because of its momentous effects on the overall MOF framework, which consequently affects the electrocatalytic performance of the MOF-based electrocatalysts for HER.[34]

Duan *et al.* reported on nanosheet arrays of bimetallic FeNi-MOF, which showed the best electrocatalytic activity in a basic medium (0.1 M KOH) for the hydrogen evolution reaction. FeNi-MOF showed the current density of 10 mA cm^{-2} at an overpotential of 134 mV. Furthermore, at 200 mV, it displayed stable activity up to 2000 s. Moreover, to test the overall competence of the catalyst to split the water molecules electrocatalytically, the authors assembled a two-electrode electrolyzer by employing catalysts at both cathode and anode sides. It takes 1.55 V of cell voltage to reach the current density of 10 mA cm^{-2}, and shows stability for 20 h at 1.5 V. The authors proposed that extra structural vacancies can be introduced by the existence of iron in a bimetallic catalyst system, which additionally improves the activity of FeNi-MOF. Furthermore, the electrode preparation does not need any additional binders due to the direct growth of the catalyst on the nickel foam, which evades the need for the use of insulating binders. Additionally, the Ni foam as a substrate boosts the catalyst performance by amending the mass transport of the electrolyte and product because of its microporous structure.[35]

4.2 MOFs as supports

MOF has also been selected as a support because it exhibits high pore volume and high surface area. Moreover, its catalytic active sites are highly dispersed and exposed. However, the synergetic effects between the supported catalysts and the MOF support may contrive certain astonishing mechanisms. Table 2 shows the list of MOFs (as a support)-based catalysts for HER from the literature.

Table 1 A list of pristine MOFs-based electrocatalysts for HER

Electrocatalyst	Test condition	η_{10} (mV)	Tafel slope (mV dec^{-1})	TOF (s^{-1})	Stability	Ref.
3D Nibpyfcd*H*p	0.5 M H_2SO_4	350	60	2.1×10^{-3} s^{-1}	30 hours	36
3D Cobpy(fcd*H*p)	0.5 M H_2SO_4	400	65	2.8×10^{-4} s^{-1}	2000 cycles	36
1D Zn(fcd*H*p)	0.5 M H_2SO_4	340	110	4.5×10^{-3} s^{-1}	1000 cycles	37
$Co_2(Hpycz)_4 \cdot H_2O$	0.5 M H_2SO_4	223	121	—	72 h	38
2D MOF $H_3[Ni^{III}_3(tht)_2]$	0.5 M H_2SO_4	333	80.5	—	—	39
THTA–Co $H_3[Co_3(tht)(tha)]$	0.5 M H_2SO_4	283	71	—	300 cycles	40
G/THTA–Co G/$H_3[Co_3(tht)(tha)]$	0.5 M H_2SO_4	230	70	—	400 cycles, 4 h	40
$H_3[Ni_3(tht)(tha)]$	0.5 M H_2SO_4	315	76	—	—	40
2D $Na_3[Co^{III}_3(bht)_2]$ (MOS-1)	0.05 M H_2SO_4	340	—	0.113 s^{-1}	10 h	41
3D Co/Ni-MOFs	0.5 M H_2SO_4	357	107	—	2000 cycles 96 h (Co) and 72 h (Ni)	42
Hf_{12}-CoDBP/(CNTs)	0.026 M TFA	650	178	17.7 s^{-1}	7 h	43
2D Cu MOF, $Cu_6(C_8H_4O_4)_6(H_2O)_6 \cdot H_3[P(W_3O_{10})_4]$	0.5 M H_2SO_4	660	100	113 s^{-1}	—	44
2D Co-MOFs $[Co(X_4\text{-pta})(bpy)(H_2O)_2]_n$; AB & Co–$Cl^{4-}$ MOF (3 : 4)	0.5 M H_2SO_4	283	86	—	24 h	45
Cu-MOF: HKUST-1 ED HKUST-1 HT	0.5 M H_2SO_4	590 660	183.6 222.4			46
3D: AB & Cu-BTC	0.5 M H_2SO_4	208	80	—	18 h, 2000 cycles	47
Au/Co Fe-MOFNs	0.1 M KOH		115 94	—	—	48
Pt/C (20 wt%)	0.5 M H_2SO_4	52	30	—	—	40

Open Access Article. Published on 21 June 2021. Downloaded on 2/3/2026 10:12:05 PM.
This article is licensed under a Creative Commons Attribution-NonCommercial 3.0 Unported Licence.

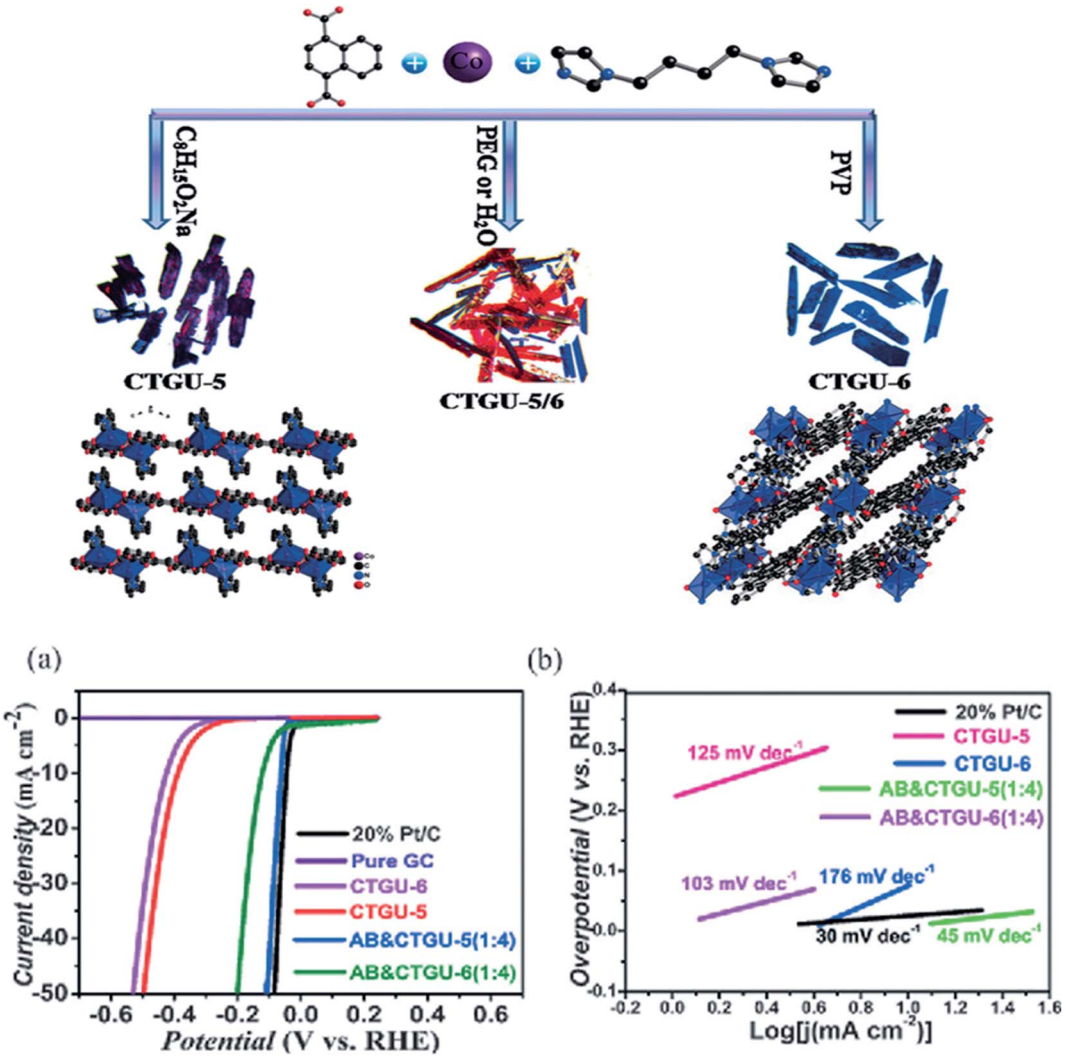

Fig. 4 Schematic illustration of the two isomeric phases of Co MOFs and their crystal structure diagrams. (a) Polarization curves for a variety of electrocatalysts in 0.5 M H_2SO_4; (b) Tafel plots of the subsequent polarization curves.[34] Exclusive rights 2017 John Wiley and Sons.

Chen *et al.* reported the anchoring of a single tungsten atom *via* pyrolysis on a carbon matrix that was already nitrogen doped, and these structures were supported on a metal–organic framework (illustrated in Fig. 5). The prepared MOF based catalysts were used for the hydrogen evolution reaction in an alkaline media. They carried out electrocatalytic studies in the presence and absence of the tungsten-modified catalysts, and compared their activity *via* polarization curve and EIS study. In

Table 2 List of MOFs (as a support)-based catalysts for HER from the literature

Sample ID	H_2 precursor	Condition	H_2 production rate (TOF)	Stability	Ref.
AuNi@MIL-101_a	$NH_3 \cdot BH_3$	Room temperature	66.2 min^{-1}	5 cycles	51
$Au_{0.28}Pd_{0.47}Co_{0.25}$/MIL-101–$NH_2$	Formic acid	25 °C	347 h^{-1}	Significant decrease after 9 cycles	54
NiPt@MIL-101	Hydrazine monohydrate	25 °C	65.2 h^{-1}	Slight decrease after 5 cycles	53
CuCo/MIL-101	$NH_3 \cdot BH_3$	Room temperature	51.7 min^{-1}	5 cycles	55
FeCo/MIL-101	—	—	50.8 min^{-1}	—	
NiCo/MIL-101	—	—	44.3 min^{-1}	—	
CuCo/MIL-101	$NH_3 \cdot BH_3$	Room temperature	19.6 min^{-1}	5 cycles	56
$Ni_{0.9}Pt_{0.1}$/MIL-101	Hydrazine borane	Room temperature	1515 h^{-1}	Slight decrease after 20 cycles	57
$Ni_{64}Pt_{36}$/MIL-96	Hydrazine monohydrate	50 °C	90 h^{-1}	4 cycles	58
$(Ni_3Pt_7)_{0.5}$–$(MnO_x)_{0.5}$/NPC-900	Hydrazine monohydrate	25 °C	120 h^{-1}	5 cycles	59
$Ni_{64}Pt_{36}$/MIL-96	Hydrazine monohydrate	25 °C	90 h^{-1}	4 cycles	58
$Ni_{0.8}Pt_{0.2}$/MIL-101–NH_2	Hydrazine monohydrate	25 °C	114.3 h^{-1}	4 cycles	60

© 2021 The Author(s). Published by the Royal Society of Chemistry

Open Access Article. Published on 21 June 2021. Downloaded on 2/3/2026 10:12:05 PM.
This article is licensed under a Creative Commons Attribution-NonCommercial 3.0 Unported Licence.

addition, they recorded the overpotential, Tafel slopes and TOF, as shown in Fig. 5a–e. The MOF-derived, nitrogen-doped, and tungsten-anchored carbon matrix exhibited a significant low overpotential value, *i.e.*, 85 mV, at a current density of 10 mA cm^{-2} with a TOF value of 6.53 s^{-1} and Tafel slope of 85 mV dec^{-1}. In contrast, the condition of no W-anchored carbon matrix-based MOF showed high TOF, overpotential and charge transfer resistance values. Moreover, the electrocatalytic study revealed that the activity of the W-anchored catalysts was comparable to that of the commercially available Pt/C in an alkaline medium (0.1 M KOH).[49]

Sun *et al.* reported on NF@Ni/C-400-700. Metal scaffolds, such as nickel foam, are often employed as substrates because they can provide high catalyst loading. The rapid mass transfer

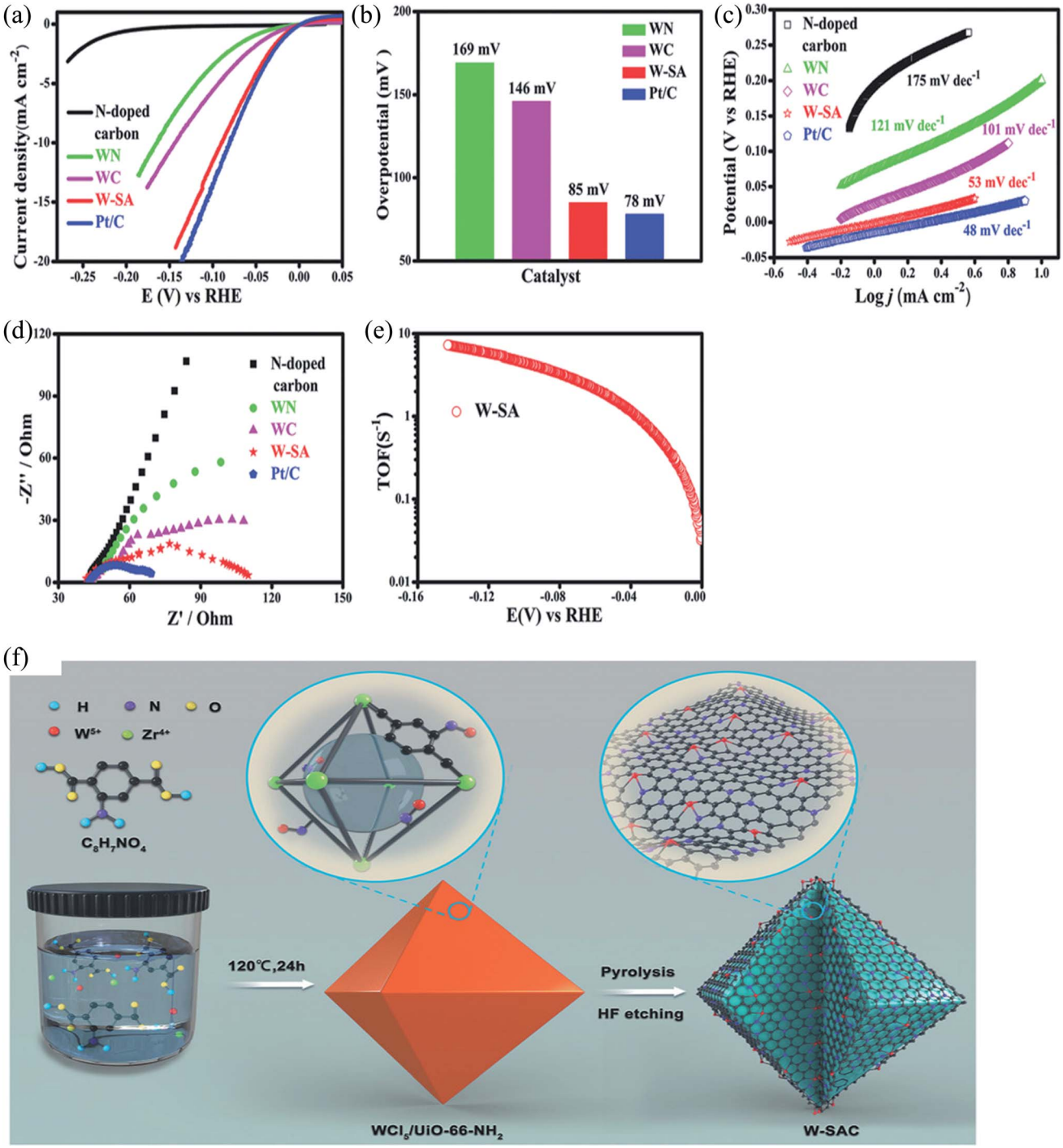

Fig. 5 HER activity of the modified electrocatalyst in alkaline media (0.1 M KOH). (a) Polarization curves of the prepared catalysts for HER, (b) comparison of the overpotential values, (c) Tafel plots and slope calculation, (d) Nyquist plots of W-SAC, (e) TOF (s^{-1}) values for W-SAC, (f) synthesis of the catalysts.[49] Exclusive rights 2018 John Wiley and Sons.

© 2021 The Author(s). Published by the Royal Society of Chemistry

Open Access Article. Published on 21 June 2021. Downloaded on 2/3/2026 10:12:05 PM.
This article is licensed under a Creative Commons Attribution-NonCommercial 3.0 Unported Licence.

enhances the catalytic activity significantly due to the lamellar structure of MOF and porous morphology of the nickel nanoparticles, which significantly encourage the access of electrolytes with enhanced mass transportation, resulting in expedited reaction kinetics.

The catalysts were synthesized *via* solvothermal method, and then calcined at different temperatures (such as 400–700 °C) under argon and hydrogen atmosphere. Among all the prepared catalysts, such as the NF@Ni/C-400, NF@Ni/C-500, NF@Ni/C-600, and NF@Ni/C-700 catalysts, NF@Ni/C-600 exhibits a considerably high HER activity in alkaline medium (1.0 M KOH) because of the following factors and synergetic effects. First, the presence of nickel nanoparticles on the carbon nanotube tip acts as a catalytic site, where proton reduction and evaluation occur. Second, the dispersion of nickel nanoparticles is homogenous on the 2D planar sheet, which remarkably lessen the hydrogen ion diffusion length. Thus, this facilitates the hydrogen ion transportation, showing a lower overpotential value of up to 37 mV at 10 mA cm^{-2}, Tafel slope value of up to 57 mV dec^{-1} and lower charge transfer resistance value of 17.5 Ω recorded at −0.1 V *vs.* RHE, which outperformed the benchmark catalysts (*e.g.*, Pt/C). The lower activity of other catalysts, such as NF@Ni/C-400 and NF@Ni/C-500, is justified by the insufficient reduction of Ni^{2+}. Furthermore, the MOF carbonization at the calcination temperature, *i.e.*, 400 and 500 °C, may affect the kinetics of the reaction and the activity of the catalysts is thus lower for HER. As far as NF@Ni/C-700 is concerned, the lower activity is justified by Sun *et al.* in the agglomeration of the nickel nanoparticles, as indicated by Fig. 6a–c.[16]

Weng *et al.* reported on a novel nanowire electrocatalyst that included S–CoWP@(S,N)–C for the hydrogen evolution reaction, comprising a sulphur and nitrogen-doped carbon matrix with CoWP nanoparticles (also doped with sulphur). The nanowires, *i.e.*, CoW-MOF, were *in situ* prepared *via* hydrothermal method, and the fabrication route is demonstrated in Fig. 7a. To know the effect of both sulphur and nitrogen doping on the carbon matrix and only sulphur doping on the nanoparticles of CoWP, the electrochemical activity was investigated in 1 M KOH. They showed enhanced activity: at a current density of 10 mA cm^{-2}, it exhibited a low overpotential of 61 mV and the Tafel slope value

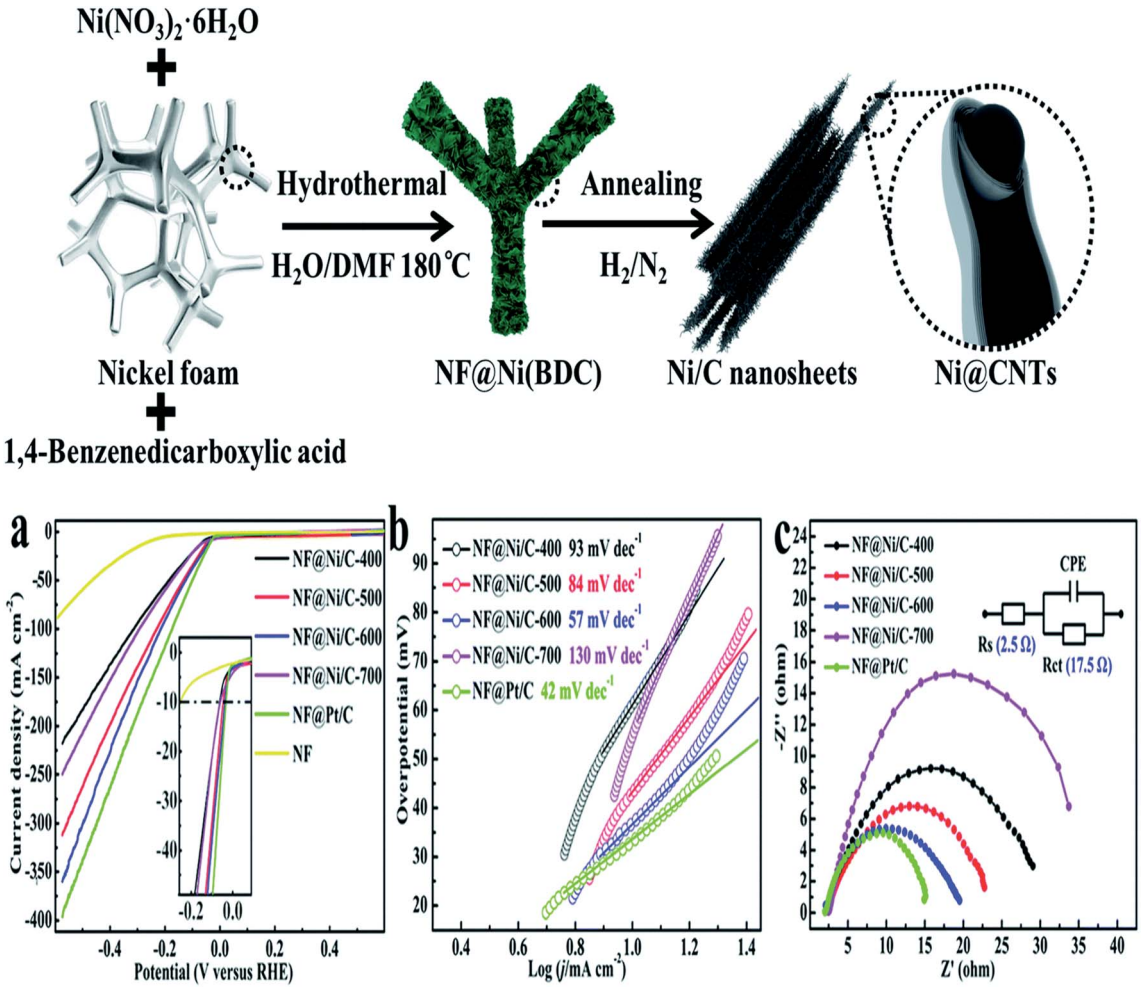

Fig. 6 HER activity of the modified electrocatalyst in an alkaline media (1.0 M KOH) synthesis of the catalysts Ni@CNTs. (a) Polarization curves of the prepared catalysts for HER, (b) comparison of the overpotential values, (c) comparative Nyquist plots of Ni@CNTs (400–700 °C).[16] Exclusive rights 2013 Royal Society of Chemistry.

© 2021 The Author(s). Published by the Royal Society of Chemistry

Open Access Article. Published on 21 June 2021. Downloaded on 2/3/2026 10:12:05 PM.
This article is licensed under a Creative Commons Attribution-NonCommercial 3.0 Unported Licence.

calculated from the Tafel plots (illustrated in Fig. 7b and c) was 55 mV dec^{-1} *vs.* RHE. This is because the S, N–C wrapping protected the S–CoWP nanoparticles well, so that their cores were prevented from oxidation, particularly during HER. Therefore, the reported catalysts are stable and active enough in alkaline media.[50]

Zhu *et al.* reported on MIL-101 (Cr-based MOF), on which the AuNi alloy nanoparticles are immobilized for better hydrogen evolution reaction. HER is chemocatalytically achieved from ammonia borane ($NH_3 \cdot BH_3$). The selection of the MIL-101 MOF as a support is based on its stability in water and air, its large pore volume and high surface area. Furthermore, the pore size window for MIL-101 is in the 1.2–1.6 nm range, which is advantageous for the Ni and Au precursor diffusion inside the frameworks. Ammonia borane catalytic hydrolysis is done by preparing the catalyst suspension in distilled water, and the considered concentration of $NH_3 \cdot BH_3$ is 1 mol L^{-1}. During the following chemocatalytic reaction, hydrogen gas is evolved, which is measured *via* water molecule displacement in a gas burette. The respective rate of hydrogen evolution is reported in terms of the turnover frequency (TOF), which is 66.2 min^{-1}. In contrast to the single metal-based MIL-101 (such as Ni@MIL-101 and Au@MIL-101), it shows better performance. The excellent activity of AuNi@MIL-101 for HER is linked with the uniform distribution of Au and Ni nanoparticles as a result of its confined growth inside the MIL-101 pore, and shows considerable stability during performance for up to five cycles.[51]

Cheng *et al.* also reported a similar immobilization of alloy nanoparticles on the MIL-101 MOF support, but the changes are the number and type of metals, the amine-modified MIL-101 as the MOF support, and AuPdCo as the incorporated metal alloys. HER is chemocatalytically achieved from formic acid, and its catalytic hydrolysis is done by preparing an aqueous solution of sodium formate and formic acid in a flask that already contains the catalyst. The respective rate of hydrogen evolution is measured at 25 °C in terms of the turnover frequency (TOF), which is 347 h^{-1}. This is excellent performance of a trimetallic nanoparticle (*i.e.*, AuPdCo) confinement within the framework pores, and in the presence of amine groups on a framework. Moreover, the presence of formic acid will lead to various coordination intermediates, such as (H_2NH^+–CoAuPd–$OOCH^-$), which generate CO_2 with the desorption of H^+ from the metal hydride H_2NH^+–CoAuPd–H^-. However, an additional step is needed for the separation of hydrogen from carbon dioxide, as both gases are produced in an equal molar quantity during the formic acid decomposition.[52]

In addition to the above mentioned bi- and trimetallic-based MIL-101 MOFs, a similar work was reported by Cao *et al.* that uses bimetallic, *i.e.*, NiPt nanoparticle immobilization inside the pores of MIL-101 for the hydrogen evolution reaction. HER is chemocatalytically achieved from hydrazine monohydrate,

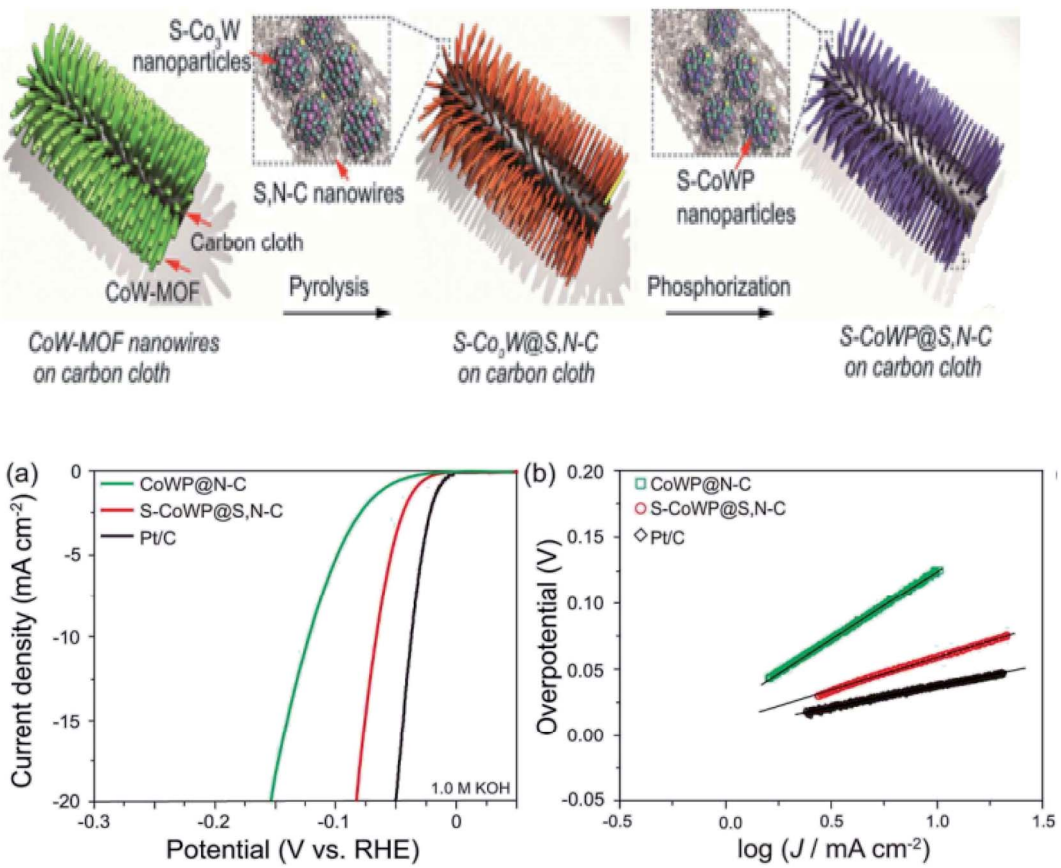

Fig. 7 HER activity of the modified electrocatalyst in an alkaline media (0.1 M KOH) synthesis of the catalysts. (a) Polarization curves, (b) comparison of overpotential values.[50] Exclusive rights 2018 ACS publications.

Open Access Article. Published on 21 June 2021. Downloaded on 2/3/2026 10:12:05 PM.
This article is licensed under a Creative Commons Attribution-NonCommercial 3.0 Unported Licence.

and its catalytic hydrolysis is done by preparing an alkaline solution of sodium hydroxide. Hydrazine hydrate is also added to the sodium hydroxide solution. The respective rate of hydrogen evolution is measured at two different temperatures (25 and 50 °C), which results in a turnover frequency of 65.2 h^{-1} (25 °C) and 375.1 h^{-1} (50 °C), respectively. Moreover, there is a slight decrease in the performance of the catalyst after 5 cycles of processes.

Likewise, MIL-101 exhibits superior detention functions. There are a number of other reports that use MIL-101 and amine-modified MIL-101 as a supporting framework, *i.e.*, for NiCo, for NiPt and others. Moreover, other reported MOFs frameworks as a support for NiPt to perform the chemocatalytic hydrogen evolution reaction, including ZIF-8 and MIL-96, are given in the literature and show superior activity for HER.[53]

4.3 MOF derivatives

In contrast to the applications offered by MOFs utilized as a support or employed as pristine MOFs, more attention has been devoted by the researchers on the deployment of MOFs as

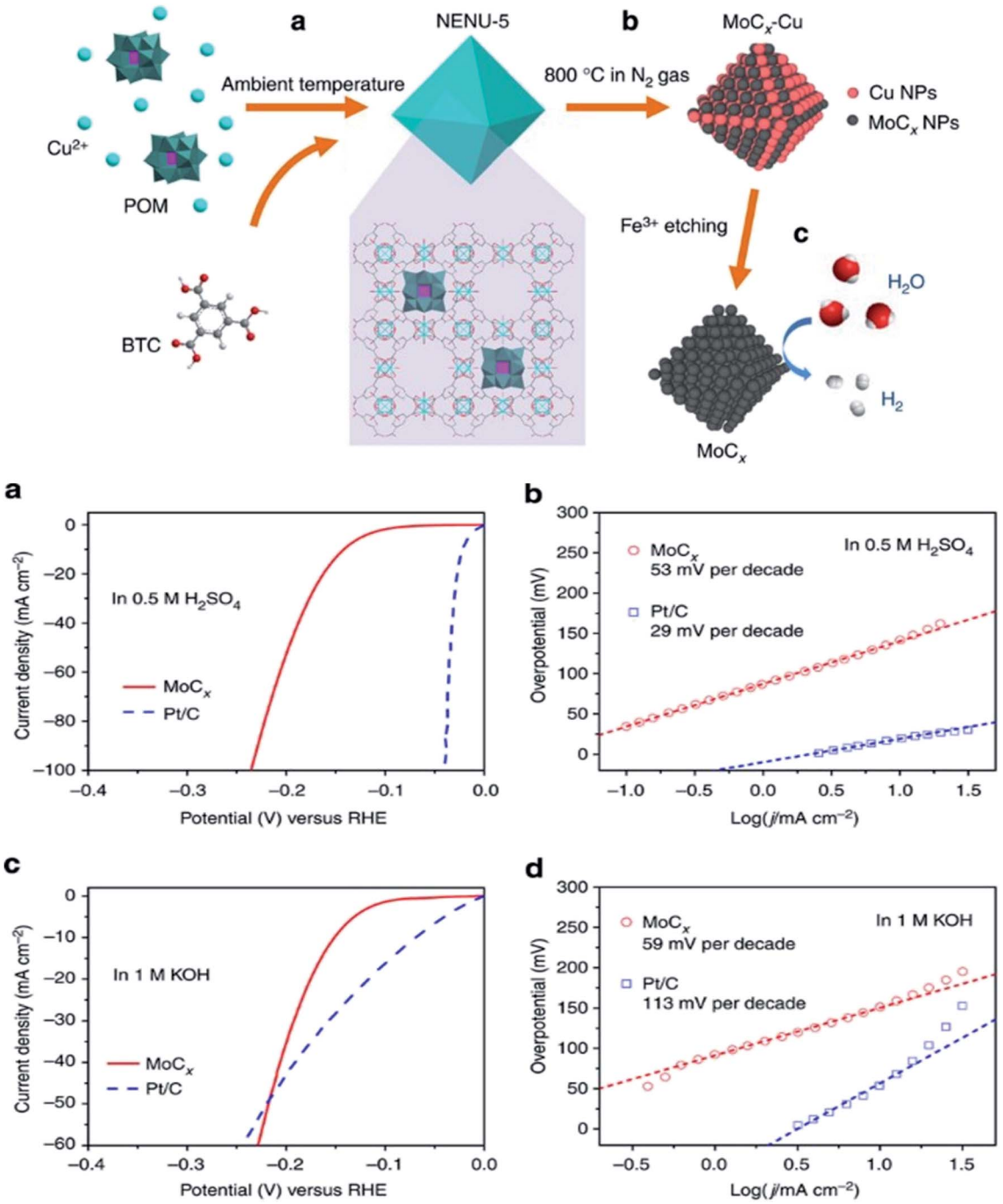

Fig. 8 Synthesis scheme of NENU-5, MoC_x–Cu; (a and b) polarization curves and Tafel plots in 0.5 H_2SO_4; (c and d) polarization curves and Tafel plots in 1 M KOH.[61] Exclusive rights 2015 SPRINGER NATURE.

© 2021 The Author(s). Published by the Royal Society of Chemistry

Open Access Article. Published on 21 June 2021. Downloaded on 2/3/2026 10:12:05 PM.
This article is licensed under a Creative Commons Attribution-NonCommercial 3.0 Unported Licence.

precursors to fabricate a wide variety of catalysts based on metals with definite designed structures and chemical components. MOFs as a precursor can harmoniously bring a pleasing surprise in structural alteration that improves the electrocatalytic performances as HER catalysts.

Wu *et al.* reported on porous MoC_x nano-octahedrons-based HER catalysts prepared from Cu-MOF ($Cu_3(BTC)_2(H_2O)_3$, BTC = benzene-1,3,5-tricarboxylate) with $H_3PMo_{12}O_{40}$ (polyoxometalate units) as guest molecules. The following MOF precursors were designed as NENU-5 ($[Cu_2(BTC)_{4/3}(H_2O)_2]_6[H_3PMo_{12}O_{40}]$). In nitrogen gas flow, the direct pyrolysis of NENU-5 is done. As a result, molybdenum carbide (MoC_x) is synthesized, elemental Cu is initially present in the carbon matrix, which is removed by treating it with $FeCl_3$ solution, as illustrated in Fig. 8a. The electrocatalytic activity of the prepared MoC_x is checked for HER in alkaline and acidic media. The catalysts show splendid performance in acidic and alkaline media, such as in acidic media (0.5 M H_2SO_4). It needed an overpotential of 142 mV to attain the current density of up to 10 mA cm^{-2} and consequent Tafel slope of up to 53 mV dec^{-1}, as illustrated in Fig. 8b and c. In alkaline media, the Tafel slope is 59 mV dec^{-1} and the overpotential is 151 mV, as illustrated in Fig. 8d and e.

At the end, it can be concluded that NENU-5 not only acts as precursors, but also precincts the growth of MoC_x. As a result, the nanosized crystals are uniformly distributed in the carbon matrix, and the prepared material shows tremendous stability in alkaline and acidic media.[61]

Yang *et al.* reported on nitrogen-doped graphene layer-encapsulated Fe–Co-based alloy nanoparticles. They are synthesized by the direct carbonation of the MOF precursor at various ranges of temperatures, *i.e.*, 600–800 °C, under the flow of nitrogen. MOF precursors, such as $Fe_3[Co(CN)_6]_2$, comprises CN– as the linker and Fe and Co are bimetallic nodes, as illustrated in Fig. 9a. At a high annealing temperature, it yields iron and cobalt-based nanoparticles that are rich in nitrogen content (8.2%) with high catalytic active sites (*i.e.*, Fe, Co) that show superb electrochemical performance for HER in acidic media. In acidic media (0.5 M H_2SO_4), it shows an overpotential of up to 262 mV for attaining a current density of 10 mA cm^{-2} and shows a slope value of 74 mV dec^{-1}. At 300 mV overpotential in the chronoamperometry test, it showed superb stability for 10 h.

The tremendous activity of the catalyst can be ascribed to subsequent qualities, such as: (i) the synergetic effect among the metals (Fe–Co) and nitrogen-doped graphene improves the catalytic performance of the prepared material, as it improves the charge transfer from the metals to the graphene site, (ii) Fe atom incorporation into the Co clusters (Co_4) modify the bond length of Co–Co, and establish new bond lengths (such as Co–Fe and Fe–Fe), which can also customize the free energy (ΔG_H), (iii) the incorporation of alloy nanoparticles *via* nitrogen-doped graphene can protect the nanoparticles from corrosion; as a result, it will enhance the stability of the catalysts.[62]

The development of a low-cost, highly active, and vastly exposed active sites-based metal–organic framework as HER electrocatalysts is an imperative and challenging step.

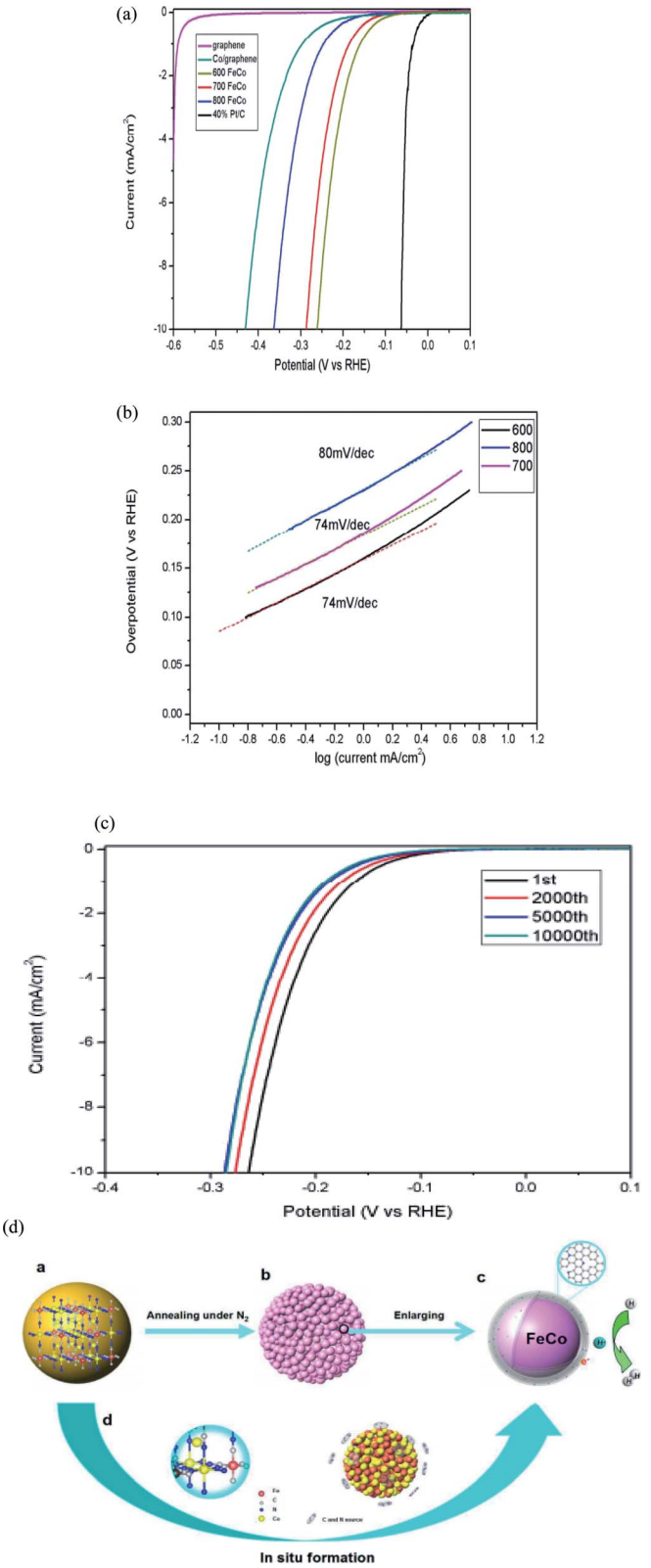

Fig. 9 (a) Polarization curves *vs.* RHE; (b) Tafel plots and (c) polarization curves; (d) synthesis scheme of FeCo alloys encapsulated in nitrogen-doped graphene layers.[62] Exclusive rights 2015 Royal Society of Chemistry.

Open Access Article. Published on 21 June 2021. Downloaded on 2/3/2026 10:12:05 PM.
This article is licensed under a Creative Commons Attribution-NonCommercial 3.0 Unported Licence.

Qiu *et al.* reported on a ruthenium-based HER electrocatalyst decorated on hierarchically porous carbon, where CuRu-MOF acts as a template during the fabrication, Cu particles are removed, and Ru particles (smaller in size) may thus be exposed and play a significant role in the HER activity. Surprisingly, at 22.7 mV of overpotential, Ru-HPC accomplished a current density of 25 mA cm^{-2} and a turnover frequency of 1.79 H_2 s^{-1} at 25 mV, which is approximately two times higher than that of the commercial Pt/C (Fig. 10a). Moreover, Ru-HPC had high active site density, *i.e.*, 0.390 × 10^{-3} mol g_{metal}^{-1} and ECSA of 385.57 m^2 g_{metal}^{-1}, which confirmed the high exposure of the Ru active sites during the electrochemical activity. Furthermore, in contrast to commercial Pt/C, it demonstrates a low Tafel slope value of 33.9 mV per decade (Fig. 10b), representing a Volmer–Tafel pathway with the recombination of the chemisorbing hydrogen atoms as the rate-limiting step. The lower

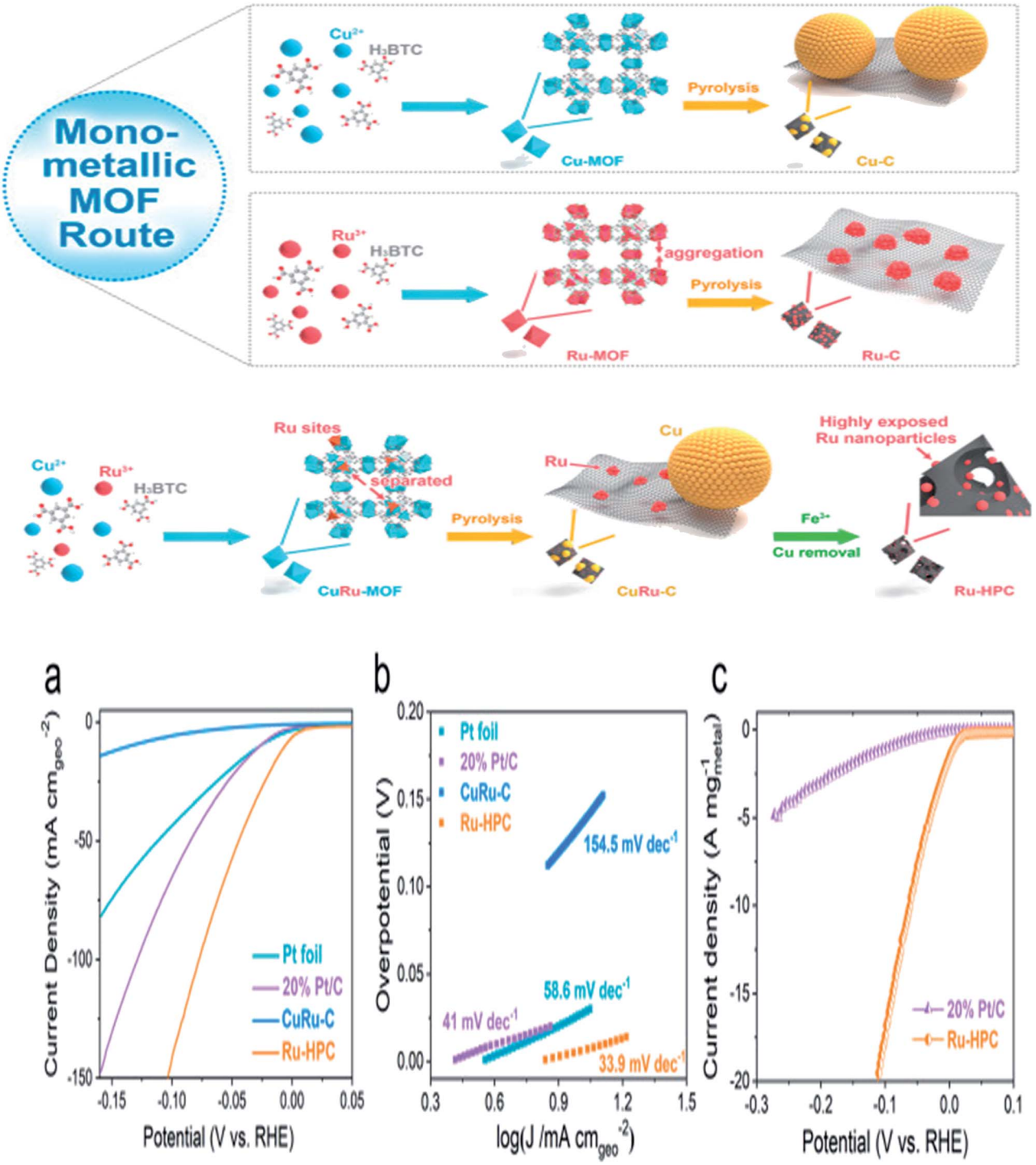

Fig. 10 Synthesis scheme of Ru-HPC; (a) polarization curves; (b) Tafel plots and (c) mass activity of Ru-HPC with Pt/C.[63] Exclusive rights 2019 ELSEVIER.

© 2021 The Author(s). Published by the Royal Society of Chemistry

Open Access Article. Published on 21 June 2021. Downloaded on 2/3/2026 10:12:05 PM. This article is licensed under a Creative Commons Attribution-NonCommercial 3.0 Unported Licence.

Tafel slope value of Ru-HPC suggested that the HER rate was augmented considerably as the overpotential increased, which is advantageous for practical application. This work presents a simple approach to manufacture high-performance metal–carbon hybrid electrocatalysts with generous bare active sites such as that of bimetallic MOFs, which should be useful to numerous other metal–carbon hybrids for a variety of electrochemical applications in the near future.[63]

In addition, MOFs such as ZIF-67 are considered to be one of the most popular precursors, and has successfully been used in the electrocatalytic hydrogen evolution reaction. In 2017 Yilmaz *et al.* reported a ZIF-67 derived system, wherein the nickel cobalt double hydroxide sulfurization will lead to the formation of NiCo-LDH/Co_9S_8, an interlayered metal sulphide system.[64] For HER, the catalyst electrocatalytic activity is tested in a basic medium, *i.e.*, 0.1 M KOH, for the attainment of a current density of 10 mA cm^{-2} and Tafel slope of 62 mV dec^{-1}. The catalyst displays an overpotential value of 142 mV, and also exhibits superior stability for 60 h under a constant potential value. This astonishing performance of the MOF-derived catalyst is due to the formation of a hollow structure, and is also due to the development of a bimetallic hydrosulphide system that plays a role in enhancing their activity for HER.

Apart from the work of Yilmaz *et al.*, many other ZIF-67-derived HER catalysts have been reported, such as nickel phosphides, porous CoP, Co@N-doped carbon nanotubes and nitrogen doped carbon.

Similarly, a list of other precursors (aside from ZIF-67) has also been reported, such as MOF-74, Co-based MOFs, Ni-based MOFs, ZIF-8 and nickel iron-based MOFs. Nickel cobalt-based MOFs are used as precursors for the preparation of different fascinating metal compounds and various other M/C-based composites for electrocatalytic water splitting.[36] Tables 3 and 4 summarise the overall HER activity of various MOFs and MOF-derived electrocatalysts.

5. Conclusions and recommendations

HER is probably the most direct and easiest way to generate high purity H_2. Many approaches have been considered for the fabrication of electrocatalysts for sustainable hydrogen production during HER. Among all the reported electrocatalysts, MOFs-based materials show remarkable activity during HER because of its high crystallinity with controllable porosity and tailorable structure. The use of MOFs-based materials as electrocatalysts for HER is because of the following reasons: (i) to replace expensive metal-based catalysts (PGM) by low-cost metals, (ii) for lowering the needed overpotential during HER, (iii) for escalating the kinetics of the reaction.

Table 3 Summary of the HER activity of various MOFs and MOF-derived electrocatalysts in acid/neutral/alkaline conditions

Catalysts	Electrolyte	Tafel slope (mV dec^{-1})	Overpotential (mV)	Ref.
CTGU-5	0.5 M H_2SO_4	−125	−388	65
CTGU-6	0.5 M H_2SO_4	−176	−425	65
AB&CTGU-5	0.5 M H_2SO_4	−45	−44	65
UiO-66-NH_2-Mo-5	0.5 M H_2SO_4	−59	−200	66
NENU-500	0.5 M H_2SO_4	−96	−237	67
NENU-501	0.5 M H_2SO_4	−137	−392	67
HUST-201	0.5 M H_2SO_4	−79	−192	68
HUST-200	0.5 M H_2SO_4	−51	−131	68
(GO 8 wt%) Cu-MOF composite		84	209 at 30 mA cm^{-2}	33
$Zn_{0.30}Co_{2.70}S_4$ polyhedra	0.5 M H_2SO_4	47.5	80	69
CoP CPHs	0.5 M H_2SO_4	51	133	70
MoC_x nano-octahedrons	0.5 M H_2SO_4	53	142	61
MoS_2/3D-NPC	0.5 M H_2SO_4	51	210	71
Au@Zn–Fe–C	0.5 M H_2SO_4	130	123	72
Layered CoP/rGO composite	0.5 M H_2SO_4	50	105	73
	1 M KOH	38	150	73
NiFeP	1.0 M KOH	−69	−178	74
Fe_3C/Mo_2C@NPGC	0.5 M H_2SO_4	−45	−98	12
Cu_3P@NPPC-650	0.5 M H_2SO_4	−76	−89	75
MoS_2/3D-NPC	0.5 M H_2SO_4	−51	−210	71
Ni_2P/C	0.5 M H_2SO_4	−113	−198	76
CoP-CNTs	0.5 M H_2SO_4	−52	−139	77
Ni–MoC_x–C (HC800)	1.0 M KOH	−83	−123	78
Mo_2C/C	1.0 M KOH	−64	−165	79
A–Ni–C	0.5 M H_2SO_4	−41	−34	80
$Cr_{0.6}Ru_{0.4}O_2$	0.5 M H_2SO_4	58	178	81
CoP@BCN-1	1.0 M KOH	−52	−215	82
CuCo@NC	0.5 M H_2SO_4	−79	−145	83
Cu_3P@NPPC-650	0.5 M H_2SO_4	−76	−89	75
Ni foam, SS mesh	1 M KOH	130, 51	1.74 V, 0.277	84
NSPC-1000	0.5 M H_2SO_4		172	85

Open Access Article. Published on 21 June 2021. Downloaded on 2/3/2026 10:12:05 PM.
This article is licensed under a Creative Commons Attribution-NonCommercial 3.0 Unported Licence.

Table 4 Summary of the HER activity of various metal-based composites in acid/neutral/alkaline conditions

Catalysts	Electrolytes	Tafel slope (mV dec^{-1})	η@j (mV@mA^{-2})	Ref.
Pt–MoS_2	0.1 M H_2SO_4	96	~ 150@10	86
ALD50Pt/NGNs	0.5 M H_2SO_4	29	50@16	87
400-SWMT/Pt	0.5 M H_2SO_4	38	27@10	88
Pt-GDY2	0.5 M H_2SO_4	38	~ 50@30	89
PtSA-NT-NF	1.0 M PBS	30	24@10	90
Pt SAs/DG	0.5 M H_2SO_4	25	23@10	91
$Mo_2TiC_2T_x$-Pt_{SA}	0.5 M H_2SO_4	30	30@10	92
Pt@PCM	0.5 M H_2SO_4	65.3	105@10	93
Pt@PCM	1.0 M KOH	73.6	139@10	93
Pt_1–MoO_{3-x}	0.5 M H_2SO_4	28.8	23.3@10	94
Pt SASs/AG	0.5 M H_2SO_4	29.33	12@10	95
SANi-PtNWs	1.0 M KOH	60.3	70@10	96
Pt1/NMC	0.5 M H_2SO_4	26	55@100	97
Pt/np-$Co_{0.85}Se$	1.0 M PBS	35	55@10	98
Pd–MoS_2	0.5 M H_2SO_4	62	78@10	99
Ru SAs@PN	0.5 M H_2SO_4	38	24@10	100
Ru@Co SAs/N–C	1.0 M KOH	30	7@10	101
Ru–MoS_2/CC	1.0 M KOH	114	41@10	102
Pt–Ru dimer	0.5 M H_2SO_4	28.9	~ 20@10	103
Fe/GD	0.5 M H_2SO_4	37.8	66@10	104
Ni/GD	0.5 M H_2SO_4	45.8	88@10	104
A–Ni–C	0.5 M H_2SO_4	41	34@10	80
Ni-doped graphene	0.5 M H_2SO_4	45	180@10	105
A–Ni@DG	0.5 M H_2SO_4	31	70@10	106
SANi-I	1.0 M KOH	34.6	60@100	107
Co–NG	0.5 M H_2SO_4	82	147@10	108
Co_1/PCN	1.0 M KOH	52	138@10	109
Co SAs/PTF-600	0.5 M H_2SO_4	50	94@10	110
$Mo_1N_1C_2$	0.5 M H_2SO_4	86	154@10	111
$W_1N_1C_3$	0.5 M H_2SO_4	58	105@10	49

For water splitting, much effort has been focused on improving the stability of the MOF-based material and its catalytic activity in alkaline and acidic media, such as: (i) the development of an unsaturated active site inside the framework; (ii) replacement of available elements in the framework by various other catalytically active elements; (iii) doping of many catalytically active elements with other elements, such as ions and nanoparticles, which may boost the stability and activity of the fabricated material; (iv) considering the chances to design a metal–organic framework with distinct functionalities, and it is necessary to incorporate the types of functional groups that are more susceptible to water splitting; (v) direct fabrication on conductive substrates, such as nickel and copper foam, and on titanium foil; (vi) composite formation by the introduction of various carbon-based components, *i.e.*, pristine graphene, carbon nanotubes, reduced graphene oxide and carbon cloth to enhance their surface area for the exposure of more active sites on the framework to speed up the mass transport efficiency between the catalyst and electrolyte.

We have undoubtedly highlighted in the previous sections how MOFs could be employed as catalysts for HER. The demand for catalysts with a high surface area and carbon support is evident. Furthermore, the chances to design MOFs composites are still there as a result of their unique physio-chemical properties, apparent stability under acidic and alkaline conditions, and the chances to promote efficiency *via* simple modification procedures that demonstrate high activity during HER. Certainly, when these issues are adequately addressed and the stable electrocatalysts in acidic and alkaline media are established, the application of MOFs will escalate water splitting as a more environmentally friendly way to produce hydrogen. There are a few recommendations that need to be addressed for enhanced production hydrogen. First, under varying working conditions, the MOF-based catalysts lost their stability. Therefore, detailed experiments are recommended to examine the changes in the catalytic sites during catalysis. Like other evaluation reactions, HER also requires a high overpotential. Therefore, it is imperative to find a suitable electrocatalyst that considerably exploits the efficiency of the process. For this purpose, it is recommended to develop a functionalized carbon-based HER catalyst with highly promising properties, such as containing abundant active sites with more controllable structural morphologies, and also having more tolerance to alkaline and acidic conditions. Similarly, it is well known that solar energy is a renewable source of energy. It is recommended to integrate these HER catalysts into different solar cells for the sustainable production of hydrogen. In addition, for an efficient electrocatalyst, extra effort is needed to understand the reaction rate-determining steps and reaction kinetics. For this purpose, different *in situ* spectroscopic techniques are used. However, they are still not well developed, and it needs more advances.

Conflicts of interest

There are no conflicts to declare.

References

1 F. Z. Song, Q. L. Zhu, X. Yang, W. W. Zhan, P. Pachfule, N. Tsumori and Q. Xu, Metal–organic framework templated porous carbon-metal oxide/reduced graphene oxide as superior support of bimetallic nanoparticles for efficient hydrogen generation from formic acid, *Adv. Energy Mater.*, 2018, **8**(1), 1701416.
2 J. Wang, M. Zhang, J. Meng, Q. Li and J. Yang, Single-and few-layer BiOI as promising photocatalysts for solar water splitting, *RSC Adv.*, 2017, **7**(39), 24446–24452.
3 Y. Xu, Y. Yao, W. Yin, J. Cao, M. Chen and X. Wei, Intrinsic defect engineered Janus MoSSe sheet as a promising photocatalyst for water splitting, *RSC Adv.*, 2020, **10**(18), 10816–10825.
4 F. Song, W. Li and Y. Sun, Metal–organic frameworks and their derivatives for photocatalytic water splitting, *Inorganics*, 2017, **5**(3), 40.
5 F. Safizadeh, E. Ghali and G. Houlachi, Electrocatalysis developments for hydrogen evolution reaction in alkaline solutions–a review, *Int. J. Hydrogen Energy*, 2015, **40**(1), 256–274.
6 (*a*) B. Ruqia and S. I. Choi, Pt and Pt–Ni$(OH)_2$ Electrodes for the Hydrogen Evolution Reaction in Alkaline Electrolytes and Their Nanoscaled Electrocatalysts, *ChemSusChem*,

© 2021 The Author(s). Published by the Royal Society of Chemistry

Open Access Article. Published on 21 June 2021. Downloaded on 2/3/2026 10:12:05 PM.
This article is licensed under a Creative Commons Attribution-NonCommercial 3.0 Unported Licence.

2018, **11**(16), 2643–2653; (*b*) Y. Wang, L. Chen, X. Yu, Y. Wang and G. Zheng, Superb Alkaline Hydrogen Evolution and Simultaneous Electricity Generation by Pt-Decorated Ni_3N Nanosheets, *Adv. Energy Mater.*, 2017, **7**(2), 1601390.

7 (*a*) J. Mahmood, F. Li, S.-M. Jung, M. S. Okyay, I. Ahmad, S.-J. Kim, N. Park, H. Y. Jeong and J.-B. Baek, An efficient and pH-universal ruthenium-based catalyst for the hydrogen evolution reaction, *Nat. Nanotechnol.*, 2017, **12**(5), 441; (*b*) N. Danilovic, R. Subbaraman, D. Strmcnik, V. Stamenkovic and N. Markovic, Electrocatalysis of the HER in acid and alkaline media, *J. Serb. Chem. Soc.*, 2013, **78**(12), 2007–2015; (*c*) W. Sheng, M. Myint, J. G. Chen and Y. Yan, Correlating the hydrogen evolution reaction activity in alkaline electrolytes with the hydrogen binding energy on monometallic surfaces, *Energy Environ. Sci.*, 2013, **6**(5), 1509–1512.

8 J. Staszak-Jirkovský, C. D. Malliakas, P. P. Lopes, N. Danilovic, S. S. Kota, K.-C. Chang, B. Genorio, D. Strmcnik, V. R. Stamenkovic and M. G. Kanatzidis, Design of active and stable Co–Mo–S_x chalcogels as pH-universal catalysts for the hydrogen evolution reaction, *Nat. Mater.*, 2016, **15**(2), 197–203.

9 J. Wang, F. Xu, H. Jin, Y. Chen and Y. Wang, Non-noble metal-based carbon composites in hydrogen evolution reaction: fundamentals to applications, *Adv. Mater.*, 2017, **29**(14), 1605838.

10 J. S. Kang, J. Kim, J. S. Kim, K. Nam, H. Jo, Y. J. Son, J. Kang, J. Jeong, H. Choe and T.-H. Kwon, Electrochemically Synthesized Mesoscopic Nickel Oxide Films as Photocathodes for Dye-Sensitized Solar Cells, *ACS Appl. Energy Mater.*, 2018, **1**(8), 4178–4185.

11 A. Eftekhari, Electrocatalysts for hydrogen evolution reaction, *Int. J. Hydrogen Energy*, 2017, **42**(16), 11053–11077.

12 J.-S. Li, Y.-J. Tang, C.-H. Liu, S.-L. Li, R.-H. Li, L.-Z. Dong, Z.-H. Dai, J.-C. Bao and Y.-Q. Lan, Polyoxometalate-based metal–organic framework-derived hybrid electrocatalysts for highly efficient hydrogen evolution reaction, *J. Mater. Chem. A*, 2016, **4**(4), 1202–1207.

13 G. Voitic and V. Hacker, Recent advancements in chemical looping water splitting for the production of hydrogen, *RSC Adv.*, 2016, **6**(100), 98267–98296.

14 L. Zhang, T. Zhang, K. Dai, L. Zhao, Q. Wei, B. Zhang and X. Xiang, Ultrafine Co_3O_4 nanolayer-shelled CoWP nanowire array: a bifunctional electrocatalyst for overall water splitting, *RSC Adv.*, 2020, **10**(49), 29326–29335.

15 A. K. Ipadeola and K. I. Ozoemena, Alkaline water-splitting reactions over Pd/Co-MOF-derived carbon obtained via microwave-assisted synthesis, *RSC Adv.*, 2020, **10**(29), 17359–17368.

16 H. Sun, Y. Lian, C. Yang, L. Xiong, P. Qi, Q. Mu, X. Zhao, J. Guo, Z. Deng and Y. Peng, A hierarchical nickel–carbon structure templated by metal–organic frameworks for efficient overall water splitting, *Energy Environ. Sci.*, 2018, **11**(9), 2363–2371.

17 H. Zhong, C. A. Campos-Roldán, Y. Zhao, S. Zhang, Y. Feng and N. Alonso-Vante, Recent advances of cobalt-based electrocatalysts for oxygen electrode reactions and hydrogen evolution reaction, *Catalysts*, 2018, **8**(11), 559.

18 F. Z. Song, X. Yang and Q. Xu, Ultrafine bimetallic Pt–Ni nanoparticles achieved by metal–organic framework templated zirconia/porous carbon/reduced graphene oxide: remarkable catalytic activity in dehydrogenation of hydrous hydrazine, *Small Methods*, 2020, **4**(1), 1900707.

19 K. G. dos Santos, C. T. Eckert, E. De Rossi, R. A. Bariccatti, E. P. Frigo, C. A. Lindino and H. J. Alves, Hydrogen production in the electrolysis of water in Brazil, a review, *Renewable Sustainable Energy Rev.*, 2017, **68**, 563–571.

20 J. Wang, T. Qiu, X. Chen, Y. Lu and W. Yang, N-doped carbon@Ni–Al_2O_3 nanosheet array@graphene oxide composite as an electrocatalyst for hydrogen evolution reaction in alkaline medium, *J. Power Sources*, 2015, **293**, 178–186.

21 T. Schmidt, V. Stamenkovic, P. Ross, Jr and N. Markovic, Temperature dependent surface electrochemistry on Pt single crystals in alkaline electrolyte Part 3. The oxygen reduction reaction, *Phys. Chem. Chem. Phys.*, 2003, **5**(2), 400–406.

22 Y. Jiao, Y. Zheng, M. Jaroniec and S. Z. Qiao, Design of electrocatalysts for oxygen-and hydrogen-involving energy conversion reactions, *Chem. Soc. Rev.*, 2015, **44**(8), 2060–2086.

23 S. Shetty, M. M. J. Sadiq, D. K. Bhat and A. C. Hegde, Electrodeposition and characterization of Ni-Mo alloy as an electrocatalyst for alkaline water electrolysis, *J. Electroanal. Chem.*, 2017, **796**, 57–65.

24 J. D. Benck, T. R. Hellstern, J. Kibsgaard, P. Chakthranont and T. F. Jaramillo, Catalyzing the hydrogen evolution reaction (HER) with molybdenum sulfide nanomaterials, *ACS Catal.*, 2014, **4**(11), 3957–3971.

25 (*a*) C. Chen, Y. Kang, Z. Huo, Z. Zhu, W. Huang, H. L. Xin, J. D. Snyder, D. Li, J. A. Herron and M. Mavrikakis, Highly crystalline multimetallic nanoframes with three-dimensional electrocatalytic surfaces, *Science*, 2014, **343**(6177), 1339–1343; (*b*) X. X. Du, Y. He, X. X. Wang and J. N. Wang, Fine-grained and fully ordered intermetallic PtFe catalysts with largely enhanced catalytic activity and durability, *Energy Environ. Sci.*, 2016, **9**(8), 2623–2632.

26 N. Yuan, Q. Jiang, J. Li and J. Tang, A review on non-noble metal based electrocatalysis for the oxygen evolution reaction, *Arabian J. Chem.*, 2020, **13**(2), 4294–4309.

27 S. Sarkar and S. C. Peter, An overview on Pd-based electrocatalysts for the hydrogen evolution reaction, *Inorg. Chem. Front.*, 2018, **5**(9), 2060–2080.

28 (*a*) H. Jin, C. Guo, X. Liu, J. Liu, A. Vasileff, Y. Jiao, Y. Zheng and S.-Z. Qiao, Emerging two-dimensional nanomaterials for electrocatalysis, *Chem. Rev.*, 2018, **118**(13), 6337–6408; (*b*) S. Trasatti and O. Petrii, Real surface area measurements in electrochemistry, *J. Electroanal. Chem.*, 1992, **327**(1–2), 353–376.

29 Y. Zheng, Y. Jiao, M. Jaroniec and S. Z. Qiao, Advancing the electrochemistry of the hydrogen-evolution reaction through combining experiment and theory, *Angew. Chem., Int. Ed.*, 2015, **54**(1), 52–65.

Open Access Article. Published on 21 June 2021. Downloaded on 2/3/2026 10:12:05 PM.
This article is licensed under a Creative Commons Attribution-NonCommercial 3.0 Unported Licence.

30 K. Aneeshkumar, J.-c. Tseng, X. Liu, J. Tian, D. Diao and J. Shen, Electrochemically dealloyed nanoporous $Fe_{40}Ni_{20}Co_{20}P_{15}C_5$ metallic glass for efficient and stable electrocatalytic hydrogen and oxygen generation, *RSC Adv.*, 2021, **11**(13), 7369–7380.

31 F. Song, W. Li, J. Yang, G. Han, T. Yan, X. Liu, Y. Rao, P. Liao, Z. Cao and Y. Sun, Interfacial sites between cobalt nitride and cobalt act as bifunctional catalysts for hydrogen electrochemistry, *ACS Energy Lett.*, 2019, **4**(7), 1594–1601.

32 F. Sun, Q. Li, H. Xue and H. Pang, Pristine Transition-Metal-Based Metal-Organic Frameworks for Electrocatalysis, *ChemElectroChem*, 2019, **6**(5), 1273–1299.

33 M. Jahan, Z. Liu and K. P. Loh, A Graphene oxide and copper-centered metal organic framework composite as a tri-functional catalyst for HER, OER, and ORR, *Adv. Funct. Mater.*, 2013, **23**(43), 5363–5372.

34 Y. P. Wu, W. Zhou, J. Zhao, W. W. Dong, Y. Q. Lan, D. S. Li, C. Sun and X. Bu, Surfactant-Assisted Phase-Selective Synthesis of New Cobalt MOFs and Their Efficient Electrocatalytic Hydrogen Evolution Reaction, *Angew. Chem.*, 2017, **129**(42), 13181–13185.

35 J. Duan, S. Chen and C. Zhao, Ultrathin metal-organic framework array for efficient electrocatalytic water splitting, *Nat. Commun.*, 2017, **8**(1), 1–7.

36 V. Khrizanforova, R. Shekurov, V. Miluykov, M. Khrizanforov, V. Bon, S. Kaskel, A. Gubaidullin, O. Sinyashin and Y. Budnikova, 3D Ni and Co redox-active metal–organic frameworks based on ferrocenyl diphosphinate and 4,4′-bipyridine ligands as efficient electrocatalysts for the hydrogen evolution reaction, *Dalton Trans.*, 2020, **49**(9), 2794–2802.

37 R. Shekurov, V. Khrizanforova, L. Gilmanova, M. Khrizanforov, V. Miluykov, O. Kataeva, Z. Yamaleeva, T. Burganov, T. Gerasimova and A. Khamatgalimov, Zn and Co redox active coordination polymers as efficient electrocatalysts, *Dalton Trans.*, 2019, **48**(11), 3601–3609.

38 Y.-C. Zhou, W.-W. Dong, M.-Y. Jiang, Y.-P. Wu, D.-S. Li, Z.-F. Tian and J. Zhao, A new 3D 8-fold interpenetrating 66-dia topological Co-MOF: syntheses, crystal structure, magnetic properties and electrocatalytic hydrogen evolution reaction, *J. Solid State Chem.*, 2019, **279**, 120929.

39 R. Dong, M. Pfeffermann, H. Liang, Z. Zheng, X. Zhu, J. Zhang and X. Feng, Large-area, free-standing, two-dimensional supramolecular polymer single-layer sheets for highly efficient electrocatalytic hydrogen evolution, *Angew. Chem., Int. Ed.*, 2015, **54**(41), 12058–12063.

40 R. Dong, Z. Zheng, D. C. Tranca, J. Zhang, N. Chandrasekhar, S. Liu, X. Zhuang, G. Seifert and X. Feng, Immobilizing molecular metal dithiolene–diamine complexes on 2D metal–organic frameworks for electrocatalytic H2 production, *Chem.–Eur. J.*, 2017, **23**(10), 2255–2260.

41 A. J. Clough, J. W. Yoo, M. H. Mecklenburg and S. C. Marinescu, Two-dimensional metal–organic surfaces for efficient hydrogen evolution from water, *J. Am. Chem. Soc.*, 2015, **137**(1), 118–121.

42 X. Wang, J.-Y. Luo, J.-W. Tian, D.-D. Huang, Y.-P. Wu, S. Li and D.-S. Li, Two new 3D isostructural Co/Ni-MOFs showing four-fold polyrotaxane-like networks: synthesis, crystal structures and hydrogen evolution reaction, *Inorg. Chem. Commun.*, 2018, **98**, 141–144.

43 D. Micheroni, G. Lan and W. Lin, Efficient electrocatalytic proton reduction with carbon nanotube-supported metal–organic frameworks, *J. Am. Chem. Soc.*, 2018, **140**(46), 15591–15595.

44 A. Hu, Q. Pang, C. Tang, J. Bao, H. Liu, K. Ba, S. Xie, J. Chen, J. Chen and Y. Yue, Epitaxial Growth and Integration of Insulating Metal–Organic Frameworks in Electrochemistry, *J. Am. Chem. Soc.*, 2019, **141**(28), 11322–11327.

45 Y.-S. Li, J.-W. Yi, J.-H. Wei, Y.-P. Wu, B. Li, S. Liu, C. Jiang, H.-G. Yu and D.-S. Li, Three 2D polyhalogenated Co (II)-based MOFs: syntheses, crystal structure and electrocatalytic hydrogen evolution reaction, *J. Solid State Chem.*, 2020, **281**, 121052.

46 X. F. Li, M. Y. Lu, H. Y. Yu, T. H. Zhang, J. Liu, J. H. Tian and R. Yang, Copper-Metal Organic Frameworks Electrodeposited on Carbon Paper as an Enhanced Cathode for the Hydrogen Evolution Reaction, *ChemElectroChem*, 2019, **6**(17), 4507–4510.

47 X. Wang, W. Zhou, Y.-P. Wu, J.-W. Tian, X.-K. Wang, D.-D. Huang, J. Zhao and D.-S. Li, Two facile routes to an AB&Cu-MOF composite with improved hydrogen evolution reaction, *J. Alloys Compd.*, 2018, **753**, 228–233.

48 S. S. Wang, L. Jiao, Y. Qian, W. C. Hu, G. Y. Xu, C. Wang and H. L. Jiang, Boosting Electrocatalytic Hydrogen Evolution over Metal–Organic Frameworks by Plasmon-Induced Hot-Electron Injection, *Angew. Chem., Int. Ed.*, 2019, **58**(31), 10713–10717.

49 W. Chen, J. Pei, C. T. He, J. Wan, H. Ren, Y. Wang, J. Dong, K. Wu, W. C. Cheong and J. Mao, Single Tungsten Atoms Supported on MOF-Derived N-Doped Carbon for Robust Electrochemical Hydrogen Evolution, *Adv. Mater.*, 2018, **30**(30), 1800396.

50 B. Weng, C. R. Grice, W. Meng, L. Guan, F. Xu, Y. Yu, C. Wang, D. Zhao and Y. Yan, Metal–Organic Framework-Derived CoWP@C Composite Nanowire Electrocatalyst for Efficient Water Splitting, *ACS Energy Lett.*, 2018, **3**(6), 1434–1442.

51 Q.-L. Zhu, J. Li and Q. Xu, Immobilizing metal nanoparticles to metal–organic frameworks with size and location control for optimizing catalytic performance, *J. Am. Chem. Soc.*, 2013, **135**(28), 10210–10213.

52 F.-Z. Song, Q.-L. Zhu, N. Tsumori and Q. Xu, Diamine-alkalized reduced graphene oxide: immobilization of sub-2 nm palladium nanoparticles and optimization of catalytic activity for dehydrogenation of formic acid, *ACS Catal.*, 2015, **5**(9), 5141–5144.

53 N. Cao, L. Yang, H. Dai, T. Liu, J. Su, X. Wu, W. Luo and G. Cheng, Immobilization of ultrafine bimetallic Ni–Pt nanoparticles inside the pores of metal–organic frameworks as efficient catalysts for dehydrogenation of

© 2021 The Author(s). Published by the Royal Society of Chemistry

Open Access Article. Published on 21 June 2021. Downloaded on 2/3/2026 10:12:05 PM.
This article is licensed under a Creative Commons Attribution-NonCommercial 3.0 Unported Licence.

alkaline solution of hydrazine, *Inorg. Chem.*, 2014, **53**(19), 10122–10128.

54 J. Cheng, X. Gu, P. Liu, T. Wang and H. Su, Controlling catalytic dehydrogenation of formic acid over low-cost transition metal-substituted AuPd nanoparticles immobilized by functionalized metal–organic frameworks at room temperature, *J. Mater. Chem. A*, 2016, **4**(42), 16645–16652.

55 P. Liu, X. Gu, K. Kang, H. Zhang, J. Cheng and H. Su, Highly efficient catalytic hydrogen evolution from ammonia borane using the synergistic effect of crystallinity and size of noble-metal-free nanoparticles supported by porous metal–organic frameworks, *ACS Appl. Mater. Interfaces*, 2017, **9**(12), 10759–10767.

56 J. Li, Q.-L. Zhu and Q. Xu, Non-noble bimetallic CuCo nanoparticles encapsulated in the pores of metal–organic frameworks: synergetic catalysis in the hydrolysis of ammonia borane for hydrogen generation, *Catal. Sci. Technol.*, 2015, **5**(1), 525–530.

57 Z. Zhang, S. Zhang, Q. Yao, X. Chen and Z.-H. Lu, Controlled synthesis of MOF-encapsulated NiPt nanoparticles toward efficient and complete hydrogen evolution from hydrazine borane and hydrazine, *Inorg. Chem.*, 2017, **56**(19), 11938–11945.

58 A. K. Singh and Q. Xu, Metal–Organic Framework Supported Bimetallic Ni˙ Pt Nanoparticles as High-performance Catalysts for Hydrogen Generation from Hydrazine in Aqueous Solution, *ChemCatChem*, 2013, **5**(10), 3000–3004.

59 B. Xia, T. Liu, W. Luo and G. Cheng, NiPt–MnO_x supported on N-doped porous carbon derived from metal–organic frameworks for highly efficient hydrogen generation from hydrazine, *J. Mater. Chem. A*, 2016, **4**(15), 5616–5622.

60 L. Wen, X. Du, J. Su, W. Luo, P. Cai and G. Cheng, Ni–Pt nanoparticles growing on metal organic frameworks (MIL-96) with enhanced catalytic activity for hydrogen generation from hydrazine at room temperature, *Dalton Trans.*, 2015, **44**(13), 6212–6218.

61 H. B. Wu, B. Y. Xia, L. Yu, X.-Y. Yu and X. W. D. Lou, Porous molybdenum carbide nano-octahedrons synthesized via confined carburization in metal-organic frameworks for efficient hydrogen production, *Nat. Commun.*, 2015, **6**(1), 1–8.

62 Y. Yang, Z. Lun, G. Xia, F. Zheng, M. He and Q. Chen, Non-precious alloy encapsulated in nitrogen-doped graphene layers derived from MOFs as an active and durable hydrogen evolution reaction catalyst, *Energy Environ. Sci.*, 2015, **8**(12), 3563–3571.

63 T. Qiu, Z. Liang, W. Guo, S. Gao, C. Qu, H. Tabassum, H. Zhang, B. Zhu, R. Zou and Y. Shao-Horn, Highly exposed ruthenium-based electrocatalysts from bimetallic metal-organic frameworks for overall water splitting, *Nano Energy*, 2019, **58**, 1–10.

64 G. Yilmaz, K. M. Yam, C. Zhang, H. J. Fan and G. W. Ho, In situ transformation of MOFs into layered double hydroxide embedded metal sulfides for improved electrocatalytic and supercapacitive performance, *Adv. Mater.*, 2017, **29**(26), 1606814.

65 Y. Wu, W. Zhou, J. Zhao, W. Dong, Y. Lan, D. Li, C. Sun and X. Bu, *Angew. Chem., Int. Ed.*, 2017, **56**, 13001–13005; *Angew. Chem.*, 2017, **129**, 13181–13185.

66 X. Dai, M. Liu, Z. Li, A. Jin, Y. Ma, X. Huang, H. Sun, H. Wang and X. Zhang, Molybdenum polysulfide anchored on porous Zr-metal organic framework to enhance the performance of hydrogen evolution reaction, *J. Phys. Chem. C*, 2016, **120**(23), 12539–12548.

67 J.-S. Qin, D.-Y. Du, W. Guan, X.-J. Bo, Y.-F. Li, L.-P. Guo, Z.-M. Su, Y.-Y. Wang, Y.-Q. Lan and H.-C. Zhou, Ultrastable polymolybdate-based metal–organic frameworks as highly active electrocatalysts for hydrogen generation from water, *J. Am. Chem. Soc.*, 2015, **137**(22), 7169–7177.

68 L. Zhang, S. Li, C. J. Gómez-García, H. Ma, C. Zhang, H. Pang and B. Li, Two novel polyoxometalate-encapsulated metal–organic nanotube frameworks as stable and highly efficient electrocatalysts for hydrogen evolution reaction, *ACS Appl. Mater. Interfaces*, 2018, **10**(37), 31498–31504.

69 Z.-F. Huang, J. Song, K. Li, M. Tahir, Y.-T. Wang, L. Pan, L. Wang, X. Zhang and J.-J. Zou, Hollow cobalt-based bimetallic sulfide polyhedra for efficient all-pH-value electrochemical and photocatalytic hydrogen evolution, *J. Am. Chem. Soc.*, 2016, **138**(4), 1359–1365.

70 M. Xu, L. Han, Y. Han, Y. Yu, J. Zhai and S. Dong, Porous CoP concave polyhedron electrocatalysts synthesized from metal–organic frameworks with enhanced electrochemical properties for hydrogen evolution, *J. Mater. Chem. A*, 2015, **3**(43), 21471–21477.

71 Y. Liu, X. Zhou, T. Ding, C. Wang and Q. Yang, 3D architecture constructed via the confined growth of MoS_2 nanosheets in nanoporous carbon derived from metal–organic frameworks for efficient hydrogen production, *Nanoscale*, 2015, **7**(43), 18004–18009.

72 J. Lu, W. Zhou, L. Wang, J. Jia, Y. Ke, L. Yang, K. Zhou, X. Liu, Z. Tang and L. Li, Core-Shell Nanocomposites Based on Gold Porous Carbons Derived from Metal-Organic Frameworks as Efficient Dual Catalysts for Oxygen Reduction and Hydrogen Evolution Reactions, *ACS Catal.*, 2016, **6**, 1045–1053.

73 L. Jiao, Y.-X. Zhou and H.-L. Jiang, Metal–organic framework-based CoP/reduced graphene oxide: high-performance bifunctional electrocatalyst for overall water splitting, *Chem. Sci.*, 2016, **7**(3), 1690–1695.

74 Y. Du, Z. Wang, H. Li, Y. Han, Y. Liu, Y. Yang, Y. Liu and L. Wang, Controllable synthesized CoP-MP (M = Fe, Mn) as efficient and stable electrocatalyst for hydrogen evolution reaction at all pH values, *Int. J. Hydrogen Energy*, 2019, **44**(36), 19978–19985.

75 R. Wang, X. Y. Dong, J. Du, J. Y. Zhao and S. Q. Zang, MOF-Derived bifunctional Cu_3P nanoparticles coated by a N, P-codoped carbon shell for hydrogen evolution and oxygen reduction, *Adv. Mater.*, 2018, **30**(6), 1703711.

Open Access Article. Published on 21 June 2021. Downloaded on 2/3/2026 10:12:05 PM.
This article is licensed under a Creative Commons Attribution-NonCommercial 3.0 Unported Licence.

76 S. He, S. He, X. Bo, Q. Wang, F. Zhan, Q. Wang and C. Zhao, Porous Ni_2P/C microrods derived from microwave-prepared MOF-74-Ni and its electrocatalysis for hydrogen evolution reaction, *Mater. Lett.*, 2018, **231**, 94–97.

77 C. Wu, Y. Yang, D. Dong, Y. Zhang and J. Li, In situ coupling of CoP polyhedrons and carbon nanotubes as highly efficient hydrogen evolution reaction electrocatalyst, *Small*, 2017, **13**(15), 1602873.

78 H. Sun, X. Xu, Z. Yan, X. Chen, F. Cheng, P. S. Weiss and J. Chen, Porous multishelled Ni_2P hollow microspheres as an active electrocatalyst for hydrogen and oxygen evolution, *Chem. Mater.*, 2017, **29**(19), 8539–8547.

79 M. Qamar, A. Adam, B. Merzougui, A. Helal, O. Abdulhamid and M. Siddiqui, Metal–organic framework-guided growth of Mo_2C embedded in mesoporous carbon as a high-performance and stable electrocatalyst for the hydrogen evolution reaction, *J. Mater. Chem. A*, 2016, **4**(41), 16225–16232.

80 L. Fan, P. F. Liu, X. Yan, L. Gu, Z. Z. Yang, H. G. Yang, S. Qiu and X. Yao, Atomically isolated nickel species anchored on graphitized carbon for efficient hydrogen evolution electrocatalysis, *Nat. Commun.*, 2016, **7**(1), 1–7.

81 Y. Lin, Z. Tian, L. Zhang, J. Ma, Z. Jiang, B. J. Deibert, R. Ge and L. Chen, Chromium-ruthenium oxide solid solution electrocatalyst for highly efficient oxygen evolution reaction in acidic media, *Nat. Commun.*, 2019, **10**(1), 1–13.

82 H. Tabassum, W. Guo, W. Meng, A. Mahmood, R. Zhao, Q. Wang and R. Zou, Metal-organic frameworks derived cobalt phosphide architecture encapsulated into B/N Co-doped graphene nanotubes for all pH value electrochemical hydrogen evolution, *Adv. Energy Mater.*, 2017, **7**(9), 1601671.

83 M. Kuang, Q. Wang, P. Han and G. Zheng, Cu, Co-embedded N-enriched mesoporous carbon for efficient oxygen reduction and hydrogen evolution reactions, *Adv. Energy Mater.*, 2017, **7**(17), 1700193.

84 X. Hu, X. Tian, Y.-W. Lin and Z. Wang, Nickel foam and stainless steel mesh as electrocatalysts for hydrogen evolution reaction, oxygen evolution reaction and overall water splitting in alkaline media, *RSC Adv.*, 2019, **9**(54), 31563–31571.

85 X. Liu, J. Yu, H. Song, P. Song, R. Wang and Y. Xiong, Nitrogen and sulfur-codoped porous carbon derived from a BSA/ionic liquid polymer complex: multifunctional electrode materials for water splitting and supercapacitors, *RSC Adv.*, 2019, **9**(9), 5189–5196.

86 J. Deng, H. Li, J. Xiao, Y. Tu, D. Deng, H. Yang, H. Tian, J. Li, P. Ren and X. Bao, Triggering the electrocatalytic hydrogen evolution activity of the inert two-dimensional MoS_2 surface via single-atom metal doping, *Energy Environ. Sci.*, 2015, **8**(5), 1594–1601.

87 N. Cheng, S. Stambula, D. Wang, M. N. Banis, J. Liu, A. Riese, B. Xiao, R. Li, T.-K. Sham and L.-M. Liu, Platinum single-atom and cluster catalysis of the hydrogen evolution reaction, *Nat. Commun.*, 2016, **7**(1), 1–9.

88 M. Tavakkoli, N. Holmberg, R. Kronberg, H. Jiang, J. Sainio, E. I. Kauppinen, T. Kallio and K. Laasonen, Electrochemical activation of single-walled carbon nanotubes with pseudo-atomic-scale platinum for the hydrogen evolution reaction, *ACS Catal.*, 2017, **7**(5), 3121–3130.

89 X. P. Yin, H. J. Wang, S. F. Tang, X. L. Lu, M. Shu, R. Si and T. B. Lu, Engineering the coordination environment of single-atom platinum anchored on graphdiyne for optimizing electrocatalytic hydrogen evolution, *Angew. Chem., Int. Ed.*, 2018, **57**(30), 9382–9386.

90 L. Zhang, L. Han, H. Liu, X. Liu and J. Luo, Potential-cycling synthesis of single platinum atoms for efficient hydrogen evolution in neutral media, *Angew. Chem., Int. Ed.*, 2017, **56**(44), 13694–13698.

91 Y. Qu, B. Chen, Z. Li, X. Duan, L. Wang, Y. Lin, T. Yuan, F. Zhou, Y. Hu and Z. Yang, Thermal emitting strategy to synthesize atomically dispersed Pt metal sites from bulk Pt metal, *J. Am. Chem. Soc.*, 2019, **141**(11), 4505–4509.

92 J. Zhang, Y. Zhao, X. Guo, C. Chen, C.-L. Dong, R.-S. Liu, C.-P. Han, Y. Li, Y. Gogotsi and G. Wang, Single platinum atoms immobilized on an MXene as an efficient catalyst for the hydrogen evolution reaction, *Nat. Catal.*, 2018, **1**(12), 985–992.

93 H. Zhang, P. An, W. Zhou, B. Y. Guan, P. Zhang, J. Dong and X. W. D. Lou, Dynamic traction of lattice-confined platinum atoms into mesoporous carbon matrix for hydrogen evolution reaction, *Sci. Adv.*, 2018, **4**(1), eaao6657.

94 W. Liu, Q. Xu, P. Yan, J. Chen, Y. Du, S. Chu and J. Wang, Fabrication of a Single-Atom Platinum Catalyst for the Hydrogen Evolution Reaction: A New Protocol by Utilization of H_xMoO_{3-x} with Plasmon Resonance, *ChemCatChem*, 2018, **10**(5), 946–950.

95 S. Ye, F. Luo, Q. Zhang, P. Zhang, T. Xu, Q. Wang, D. He, L. Guo, Y. Zhang and C. He, Highly stable single Pt atomic sites anchored on aniline-stacked graphene for hydrogen evolution reaction, *Energy Environ. Sci.*, 2019, **12**(3), 1000–1007.

96 M. Li, K. Duanmu, C. Wan, T. Cheng, L. Zhang, S. Dai, W. Chen, Z. Zhao, P. Li and H. Fei, Single-atom tailoring of platinum nanocatalysts for high-performance multifunctional electrocatalysis, *Nat. Catal.*, 2019, **2**(6), 495–503.

97 H. Wei, H. Wu, K. Huang, B. Ge, J. Ma, J. Lang, D. Zu, M. Lei, Y. Yao and W. Guo, Ultralow-temperature photochemical synthesis of atomically dispersed Pt catalysts for the hydrogen evolution reaction, *Chem. Sci.*, 2019, **10**(9), 2830–2836.

98 K. Jiang, B. Liu, M. Luo, S. Ning, M. Peng, Y. Zhao, Y.-R. Lu, T.-S. Chan, F. M. de Groot and Y. Tan, Single platinum atoms embedded in nanoporous cobalt selenide as electrocatalyst for accelerating hydrogen evolution reaction, *Nat. Commun.*, 2019, **10**(1), 1–9.

99 Z. Luo, Y. Ouyang, H. Zhang, M. Xiao, J. Ge, Z. Jiang, J. Wang, D. Tang, X. Cao and C. Liu, Chemically activating MoS_2 via spontaneous atomic palladium interfacial doping towards efficient hydrogen evolution, *Nat. Commun.*, 2018, **9**(1), 1–8.

100 J. Yang, B. Chen, X. Liu, W. Liu, Z. Li, J. Dong, W. Chen, W. Yan, T. Yao and X. Duan, Efficient and robust

© 2021 The Author(s). Published by the Royal Society of Chemistry

Open Access Article. Published on 21 June 2021. Downloaded on 2/3/2026 10:12:05 PM.
This article is licensed under a Creative Commons Attribution-NonCommercial 3.0 Unported Licence.

hydrogen evolution: phosphorus nitride imide nanotubes as supports for anchoring single ruthenium sites, *Angew. Chem., Int. Ed.*, 2018, **57**(30), 9495–9500.

101 S. Yuan, Z. Pu, H. Zhou, J. Yu, I. S. Amiinu, J. Zhu, Q. Liang, J. Yang, D. He and Z. Hu, A universal synthesis strategy for single atom dispersed cobalt/metal clusters heterostructure boosting hydrogen evolution catalysis at all pH values, *Nano Energy*, 2019, **59**, 472–480.

102 D. Wang, Q. Li, C. Han, Z. Xing and X. Yang, Single-atom ruthenium based catalyst for enhanced hydrogen evolution, *Appl. Catal., B*, 2019, **249**, 91–97.

103 L. Zhang, R. Si, H. Liu, N. Chen, Q. Wang, K. Adair, Z. Wang, J. Chen, Z. Song and J. Li, Atomic layer deposited Pt-Ru dual-metal dimers and identifying their active sites for hydrogen evolution reaction, *Nat. Commun.*, 2019, **10**(1), 1–11.

104 Y. Xue, B. Huang, Y. Yi, Y. Guo, Z. Zuo, Y. Li, Z. Jia, H. Liu and Y. Li, Anchoring zero valence single atoms of nickel and iron on graphdiyne for hydrogen evolution, *Nat. Commun.*, 2018, **9**(1), 1–10.

105 H. J. Qiu, Y. Ito, W. Cong, Y. Tan, P. Liu, A. Hirata, T. Fujita, Z. Tang and M. Chen, Nanoporous graphene with single-atom nickel dopants: an efficient and stable catalyst for electrochemical hydrogen production, *Angew. Chem., Int. Ed.*, 2015, **54**(47), 14031–14035.

106 L. Zhang, Y. Jia, G. Gao, X. Yan, N. Chen, J. Chen, M. T. Soo, B. Wood, D. Yang and A. Du, Graphene defects trap atomic Ni species for hydrogen and oxygen evolution reactions, *Chem*, 2018, **4**(2), 285–297.

107 Y. Zhao, T. Ling, S. Chen, B. Jin, A. Vasileff, Y. Jiao, L. Song, J. Luo and S. Z. Qiao, Non-metal Single-Iodine-Atom Electrocatalysts for the Hydrogen Evolution Reaction, *Angew. Chem., Int. Ed.*, 2019, **58**(35), 12252–12257.

108 H. Fei, J. Dong, M. J. Arellano-Jiménez, G. Ye, N. D. Kim, E. L. Samuel, Z. Peng, Z. Zhu, F. Qin and J. Bao, Atomic cobalt on nitrogen-doped graphene for hydrogen generation, *Nat. Commun.*, 2015, **6**(1), 1–8.

109 L. Cao, Q. Luo, W. Liu, Y. Lin, X. Liu, Y. Cao, W. Zhang, Y. Wu, J. Yang and T. Yao, Identification of single-atom active sites in carbon-based cobalt catalysts during electrocatalytic hydrogen evolution, *Nat. Catal.*, 2019, **2**(2), 134–141.

110 J.-D. Yi, R. Xu, G.-L. Chai, T. Zhang, K. Zang, B. Nan, H. Lin, Y.-L. Liang, J. Lv and J. Luo, Cobalt single-atoms anchored on porphyrinic triazine-based frameworks as bifunctional electrocatalysts for oxygen reduction and hydrogen evolution reactions, *J. Mater. Chem. A*, 2019, **7**(3), 1252–1259.

111 W. Chen, J. Pei, C. T. He, J. Wan, H. Ren, Y. Zhu, Y. Wang, J. Dong, S. Tian and W. C. Cheong, Rational Design of Single Molybdenum Atoms Anchored on N-Doped Carbon for Effective Hydrogen Evolution Reaction, *Angew. Chem., Int. Ed.*, 2017, **56**(50), 16086–16090.